# Mitochondrial Function and Homeostasis Regulated by Asymmetric Arginine Dimethylation
# （非対称型アルギニンジメチル化によるミトコンドリアの機能制御）

2016

筑波大学グローバル教育院
School of Integrative and Global Majors in University of Tsukuba

Ph.D Program in Human Biology

Liang Sha

# Table of Contents

# ABSTRACT

## Mitochondrial Function and Homeostasis Regulated by Asymmetric Arginine Dimethylation

by

Liang Sha, Ph.D. candidate

University of Tsukuba, 2016

Primary Supervisor: Shoji Makino, Ph.D.

Vice Supervisor: Akiyoshi Fukamizu, Ph.D.

Margarete Heck, Ph.D.

**Purpose**

Protein Arginine Methyltransferase 1 (PRMT1) catalyzes asymmetric arginine dimethylation on cellular proteins and modulates various aspects of cellular processes, such as signal transduction, DNA repair, and transcriptional regulation. We have previously reported that *prmt-1* is an anti-ageing factor in *C. elegans* (*Cell Metab. 13*, 505-516, 2011) and accumulating evidence has shown that it is involved in a broad spectrum of ageing-related diseases, such as myocardial infarction (*Acta Histochemica 112*, 413-423, 2010) and

hypomyelination-induced neurodegenerative diseases (*J. Biol. Chem. 291*, 2237-2245, 2016). However, the physiological and pathological roles of PRMT-1 remain largely unclear because of the lack of *in vivo* investigation. In this study, we employed *C. elegans* as a model organism to explore the physiological functions of PRMT-1 at whole-organism level.

## Materials and methods

**Animals**: Bristol N2 wild-type, RB2047 *prmt-1(ok2710)*, TKB71 *trcEx71[prmt-1(+);Pmyo2::DsRed];prmt-1(ok2710)*, TKB84 *trcEx84[prmt-1G70A(+);Pmyo2::DsRed];prmt-1(ok2710)*, and SJ4100 *zcIs13[hsp-6::GFP]* were used.

**Plasmids**: Full-length cDNAs encoding *C. elegans hsp-60, atp-2, Y38F1A.6,* or *daf-16* were amplified by PCR and then cloned into pGEX-6P(5X) vector. FLAG tagged *C. elegans* PRMT-1 was inserted into pcDNA3 vector for mammalian cell expression.

**Two-dimensional electrophoresis (2-D PAGE)**: Whole body extracts from N2 or *prmt-1*(ok2710) were subjected to 2-D PAGE and followed by Western blot against ASYM24 or ASYM26 antibody to detect asymmetrically arginine-dimethylated proteins.

**GST pull-down assay and *in vitro* methylation**: Immobilized GST fusion proteins were incubated with FLAG-PRMT-1 to examine the protein-protein

interaction, or to assess the potential of being substrates in the presence of *S*-adenosyl-L-[*methyl*-$^{3}$H]methionine.

**Mitochondrial fractionation**: mitochondria were isolated by differential centrifugation.

**LC-MS/MS**: asymmetric or symmetric dimethylarginine (ADMA or SDMA) levels of mitochondrial fractions were quantified by LC-MS/MS.

***in vitro* ATP assay**: ATP producing function of mitochondria was assessed by *in vitro* ATP assay based on luciferin-luciferase reaction.

**MitoSOX staining**: mitochondrial ROS generation was examined by whole body staining with MitoSOX fluorescent probe.

**real-time RT-PCR**: expression levels of mitochondria-related or stress response genes were measured by real-time RT-PCR.

**RNAi feeding**: genes were selectively silenced by feeding the worms with HT115 *E. coli* harboring target gene fragments.

**Food avoidance assay**: worms were fed on 3.5 cm plates seeded with a limited area of normal or knockdown bacteria lawn, and the ratio of off-lawn worms was scored.

## Results

In this study, nine *in vivo* substrates of PRMT-1 were identified by two-dimensional Western blot-based proteomic analysis using *C. elegans*. The subcellular localizations of these substrates spans from extracellular matrix,

cytoplasm, nucleus, to organelles such as endoplasmic reticulum and mitochondria. Because the direct relation between PRMT-1 and mitochondrial functions has never been reported, we therefore focused on the function of PRMT-1 in mitochondria. Subcellular fractionation followed by LC-MS/MS analysis showed that PRMT-1 is almost entirely responsible for asymmetric arginine dimethylation on mitochondrial proteins. Metabolome analysis showed a global suppression of metabolism in *prmt-1* deletion mutants, however, the mitochondrial biogenesis was not seemed to be altered. Importantly, isolated mitochondria from *prmt-1*-null mutants represent compromised ATP synthesis probably due to decreased activity of oxidative phosphorylation *in vitro*. Transgenic rescue experiments demonstrate that PRMT-1-dependent asymmetric arginine dimethylation is required to prevent mitochondrial ROS production in *C. elegans*. Furthermore, *prmt-1*-null mutation causes induction of stress response genes involving xenobiotic-detoxification and innate immune defense, as well as the metabolic process and mitochondrial genes. Direct evidence for the mitochondrial stress was observed with the activation of mitochondrial unfolded protein response. As the behavioral response, *prmt-1* mutant worms exhibited food-avoidance behavior due to mitochondrial dysfunction.

## Discussion

Our discovery uncovered a novel role of PRMT-1 which facilitates the energy metabolism and also maintains the homeostasis of mitochondria by directly targeting mitochondrial proteins. These findings are expected to provide clues for understanding the physiological roles of PRMT-1 in higher organisms and add new layer of complexity to posttranslational regulation of mitochondrial function, ultimately contributing to the mechanismic or therapeutic research of mitochondria-related disorders, including cardiovascular and neurodegenerative diseases.

# ACKNOWLEDGEMENTS

I would like to take this opportunity to thank my primary supervisor, Dr. Shoji Makino, for his support throughout my studies throughout my research for the doctoral thesis. I would also like to thank my vice supervisor, Dr. Akiyoshi Fukamizu, for his guidance, encouragement, and willingness to help me grow as a scientist and pursue the academic career path. At the same time, I would like to express my appreciation to my committee members, Dr. Satoru Takahashi, Dr. Tomoaki Mizuno, and Dr. Toshiharu Yamashita, for their advices and suggestions.

Voyaging through the sea of scientific research would not have been as enjoyable if my mentor, Dr. Hiroaki Daitoku, had not been there with me. I appreciate his kindness and patience in every detail from teaching me experimental techniques to helping me find my strength of doing research independently. I am so lucky to have got enormous help from the lab mates or former lab members, Sho Araoi, Dr. Koichiro Kako, Dr. Kazumasa Hada, Dr. Yuta Kaneko, Dr. Kazuya Murata, Misuzu Hashimoto, Eszter Toth, Dr. Keiko Hirota, Dr. Yuta Takahashi, and Dr. Juri Hamada. Thank you all for great discussions and useful advices all the time. I am also grateful to have spent the two years in Dr. Yoshito Kumagai's laboratory for making me start to know the excitement of scientific research and kind considerations all the way through my growth during these five years.

Most importantly, I would like to thank my family for their constant supporting, understanding, and encouragement through this time in my life. I am also thankful for the joyful time I have spent with my friends, Jianghuang Lin, Yang Liu, Liying Pei, Wenqi Wang, and Chiyuan Huang. Finally, I would like to express my special thanks to Zhao Xu for always being there for me. Without your encouragement, I could have not made it this far.

Liang Sha

# CHAPTER 1
# INTRODUCTION

## I. Protein Arginine Methylation

### 1. Protein Arginine Methylation

Post-translational modifications provide important regulations on almost all aspects of biology. In addition to phosphorylation and acetylation, methylation is another major modification that closely controls protein function. A wide variety of methylation reactions occur at the side chains of a number of amino acid residues and at protein N and C termini (5). Arginine methylation is extensively happening on various proteins. Arginine is unique among amino acids as its guanidino group contains five potential hydrogen bond donors that are positioned for favorable interactions with biological hydrogen bond acceptors in protein-DNA or protein-RNA interactions (1-5). Methylation on arginine residues removes potential hydrogen bond donors. This chemical adduct also affects the protein-protein interactions.

Arginine methylation can be classified into three categories (5): omega-$N^G$,$N^G$-dimethy-larginine that two methyl groups are added on one of the terminal nitrogen atoms of the guanidino group; this derivative is commonly referred to as asymmetric dimethylarginine (ADMA) which is the most abundant arginine methylation in mammalian cells. The other

two forms of arginine methylation includes: omega-$N^G$,$N'^G$-dimethylarginine (SDMA) and the omega-$N^G$-monomethylarginine (MMA).

2. PRMTs

The formation of MMA, ADMA, and SDMA in mammalian cells is catalyzed by a family of protein arginine methyltransferases, namely, PRMTs. The PRMT family members share some structural features: each member harbors the characteristic motifs of seven-beta strand methyltransferases, as well as additional ‘‘double E’’ and ‘‘THW’’ sequence motifs (5). Generally, the PRMT family members are responsible for catalyzing first the formation of a MMA as an intermediate, and subsequently type I enzymes including PRMT1, -2, -3, -4, -6, and -8, further catalyze the generation of ADMA, while type II enzymes including PRMT5, PRMT7, and FBXO11 catalyzes the generation of SDMA. PRMT1, -3, -4 (CARM1), -6 and -8 additionally catalyze ADMA formation, whereas PRMT5 additionally catalyzes SDMA formation (1-5). A clear understanding of how PRMT catalytic polypeptides can be assembled into active complexes with other protein subunits in cells is needed. Although PRMT1, -3, -4 (CARM1), -5, -6, and -8 are active methyltransferases in the absence of other polypeptide species in vitro, they might also bind additional partners for their

functions *in vivo* (5). It now appears that interactions between PRMTs and their binding partners (and presumed regulatory subunits) can be transient or permanent. Since ADMA is the prevalent species in arginine methylation, and PRMT1 has been shown to be the predominant enzyme for ADMA formation in mammalian cells, PRMT1 has been closely focused in arginine methylation study.

3. Molecular Functions of Asymmetric Arginine Dimethylation

Accumulating evidence has shown that asymmetric arginine methylation is involved in a broad spectrum of cellular events, such as transcriptional regulation, RNA splicing, DNA repair, and signal transduction (1-5). The most extensively studied function of asymmetric arginine methylation is its transcriptional regulatory function for the modification on histone tail or other histone modifying enzymes. For example, the histone H4R3 site is a major target for PRMT1 methylation (ADMA) and is generally regarded as a transcriptional activating mark (5). The vast majority of PRMT substrates are associated with RNA, including heterogeneous nuclear ribonucleoproteins (hnRNPs) and ribosomal proteins. Thus, arginine methylation has been implicated in all aspects of RNA metabolism, including mRNA transcription, splicing, transport, translation, and turnover (1-5). Another important aspect of the functions of asymmetric arginine dimethylation on cellular proteins is that it

modulates signal transduction. An impressive example is the methylation of FOXO1 antagonizes the phosphorylation by Akt, which facilitates the nuclear translocation of FOXO1 and enhances the expression of its downstream genes (1).

4. Physiological and Pathological Relevance of Asymmetric Arginine Dimethylation

Although the molecular functions of asymmetric arginine dimethylation has been extensively studied, the physiological and pathological relevance of this modification remains largely unknown. It is partially because of the lack of *in vivo* evidence that the identified substrates of PRMT1 are methylated. Another point that obstructs the *in vivo* functional study of asymmetric arginine dimethylation is that the genetic deletion of PRMT1 in either mouse or fruit fly leads to an embryonic lethal phenotype. However, recently the tissue-specific knockout of PRMT-1 in mice gave important hints of its physiological and pathological relevance. For example, our previous work showed that conditional knockout of PRMT1 in central neuron system caused severe hypomyelation of mouse neuron cell, which is closely related to various neuronal degradative diseases, connecting the physiological function of PRMT1 to neuronal development (30). However, the underlying mechanisms for the phenotype was unknown in the study, due to the

undiscovered responsible substrates. Therefore, the gap between the revealed molecular functions of asymmetric arginine methylation and its physiological or pathological relevance requires the identification of *in vivo* substrates of PRMT1.

## II. Mitochondria

### 1. Mitochondria and ATP Synthesis

Mitochondria plays essential roles in cellular metabolism. It consists of outer membrane, inner membrane, the intermembrane space, and the matrix. In the matrix, tricarboxylic acid cycle (TCA) enzymes extract energy from different energy sources and store it in the electron carriers (NADH and FADH2), which then donate electrons to the inner membrane localized electron transport chain (ETC). The ETC consists of four protein machines (I–IV), which through sequential redox reactions undergo conformational changes to pump protons from the matrix into the intermembrane space (45). The proton gradient generated by complexes I, III, and IV is released through the rotary turbine-like ATP synthase machine or complex V, which drives phosphorylation of ADP to ATP (45).

On the other hand, mitochondria are the major place for cellular reactive oxygen species (ROS) generation which in mitochondria is produced as a byproduct of OXPHOS. ROS has been suggested to contribute to diseases

associated with mitochondrial dysfunction, including neurodegenerative or cardiovascular diseases.

2. Mitochondrial Stress and Unfolded Protein Response

Organisms have evolved sophisticated systems to monitor mitochondrial functions and maintain its homeostasis through communication between mitochondria and nucleus (2). One of these mitochondrial systems is a conserved protein quality control termed mitochondrial unfolded protein response ($UPR^{mt}$), in which the accumulation of unfolded protein within the mitochondrial matrix leads to the transcriptional activation of nuclear genes encoding mitochondrial chaperones and proteases to help protein folding, assembly, and clearance of defective proteins in stressed mitochondria (3–5). In *C. elegans*, disruption of mitochondrial function activates not only $UPR^{mt}$, but also xenobiotic-detoxification and pathogen-response pathways, suggesting that animals interpret an impaired mitochondrial activity as xenobiotic exposure or pathogen attack (6–8). Actually, *C. elegans* displays bacterial-avoidance behavior when mitochondria are inhibited by RNAi or an antibiotic such as antimycin even in the absence of pathogen attack (7, 8). This intrinsic protective behavior termed food-avoidance is also found in *Drosophila melanogaster* (9) and reminiscent of mammalian gastrointestinal responses to enteric pathogens that trigger nausea symptom (10).

3. Post-translational Modifications of Mitochondrial Proteins

Accumulating evidence has demonstrated that mitochondrial proteins undergo several posttranslational modifications, such as acetylation and phosphorylation (11, 12). For example, an estimated 35% of all mitochondrial proteins are acetylated with the highest enrichment in OXPHOS and tightly regulated by reversible acetylation (13). Interestingly, arginine methylation has recently emerged as new regulatory posttranslational modification in mitochondrial proteins; namely, NDUFS2, a subunit of mitochondrial complex I, is symmetrically dimethylated at arginine 85 by a predicted methyltransferase NDUFAF7 in the matrix of mitochondria and this methylation is required for assembly of complex I (14). In addition, it has been also reported that NDUFAF7-induced symmetric dimethylation of NDUFS2 is essential for normal vertebrate development (15). On the other hand, the responsible enzyme for asymmetric arginine dimethyaltion on mitochondrial proteins and the biological roles of this major arginine methylation (16, 17) in mitochondrial functions remain largely unknown.

4. Mitochondrial Diseases

A major milestone of the research for neuronal degradative or cardiovascular disorders was that the discovery of the connection between these diseases and mitochondrial dysfunction. Genetic investigation revealed that most of the mitochondria-related disorders arise from the defects in mitochondrial genome or nuclear genome (46). Indeed, most of the proteins that built the mitochondria are coded by nucleus. The tissues or cell types such as neurons, cardiac or skeletal muscle, have the most abundant mitochondria and are highly dependent on the mitochondrial bioenergetics, thus being extremely sensitive to mitochondrial dysfunction. Mitochondria-related diseases can be categorized into three classes: primary mitochondrial DNA mutations such as Pearson syndrome, mitochondrial-protein-coding nuclear gene mutations such as Leigh's syndrome, and mutations in mitochondrial regulatory genes such as Parkinson's disease (46). Interestingly, the gene ontology (GO) analysis showed that the acetylated mitochondrial proteins are largely enriched in metabolic pathways related to mitochondrial diseases (20). Considering that abnormality with PRMT1 is related with neurodegradative or cardiovascular diseases, it is possible that PRMT1 plays roles in mitochondrial functions.

# CHAPTER 2
# MATERIALS AND METHODS

***C. elegans* strains.** All strains were maintained and handled according to standard methods. Briefly, nematodes were maintained on NGM OP50 plates at 20°C. Bristol N2 wild-type, RB2047 *prmt-1(ok2710)*, and SJ4100 *zcIs13[hsp-6::GFP]* were obtained from the Caenorhabditis Genetics Center and the *prmt-1(ok2710)* mutant was outcrossed to N2 three times (18). The extrachromosomal *prmt-1* wild-type and G70A mutant-overexpressing lines in *prmt-1(ok2710)* background were TKB71 *trcEx71[prmt-1(+);Pmyo2::DsRed];prmt-1(ok2710)* and TKB84 *trcEx84[prmt-1G70A(+);Pmyo2::DsRed];prmt-1(ok2710)*, respectively (19).

**Feeding RNAi.** For RNAi constructs against *prmt-1* and *isp-1*, the 500 bp of each coding sequence was amplified by PCR and cloned into L4440 vector. The following primers were used: *prmt-1* RNAi, the forward (5'-ACCTTACCATGGCAGCTTCTCCGTGACAA-3') and the reverse (5'-GTATTCTGCAGCTTGGGGGTGTTTCGA-3'); *isp-1* RNAi, the forward (5'-ACCTTACCATGGCAGCTTCTCCGTGACAA-3') and the reverse (5'-GTATTCTGCAGCTTGGGGGTGTTTCGA-3'). The RNAi clones against *prmt-5*, *inx-17*, and *thoc-2* were obtained from the Ahringer library. All RNAi constructs were transformed into HT115 *E. coli* and then seeded onto NGM

plates containing 25 μg/ml carbenicillin and 1 mM IPTG for feeding RNAi experiments.

**Plasmid construction and antibodies.** Full-length cDNAs encoding *C. elegans hsp-60, atp-2, and Y38F1A.6* were amplified by PCR and then cloned into pGEX-6P(5X) vector. Expression vectors for *C. elegans daf-16* and *prmt-1* were described previously (9). The following antibodies were purchased: anti-dimethyl-Arginine Antibody, asymmetric (ASYM24) from Merck Millipore; anti-dimethyl-Arginine Antibody, asymmetric (ASYM26) from EpiCypher; anti-α-Tubulin (T5168) and anti-FLAG M2 (F1804) from Sigma-Aldrich; anti-GFP (#2956) and anti-Histone H3 (#4499) from Cell Signaling Technology; anti-ATP5A (ab14748) and anti-ATPB (ab14730) from abcam. A rabbit polyclonal antibody against PRMT-1 was raised by using synthetic peptide described previously (9).

**GST pull-down assay.** GST fusion proteins were expressed in BL-21 *E. coli* by using the pGEX vector system. GST alone or GST-fused proteins immobilized on glutathione-Sepharose 4B were incubated with HEK293T cell extracts expressing FLAG-PRMT-1 in binding buffer (50 mM Hepes, pH7.9/ 150 mM NaCl/ 0.1% TritonX-100/ protease inhibitors). After incubation for 4 hrs at 4°C, the beads were washed three times with the same buffer, and

proteins were analyzed by Coomassie Brilliant Blue staining and Western blotting with anti-FLAG antibody.

***In vitro* methylation assay.** FLAG-tagged PRMT1 was immunoprecipitated from HEK293T cells with anti-FLAG M2 affinity gel, and then eluted with FLAG peptide. Eluted PRMT-1 was combined with GST alone or GST-tagged HSP-60, ATP2, and Y38F1A.6 in the presence of 5 μCi of *S*-adenosyl-L-[*methyl*-$^{3}$H]methionine (NET155V, specific activity 666 GBq/mmol; PerkinElmer) in 30 μl of PBS, and reactions were incubated for 3 h at 30°C. After washing the beads, the reaction products were resolved by SDS-PAGE, and radioactively labeled proteins were visualized by fluorography with Amplify fluorographic reagent (GE Healthcare).

**Two-dimensional Western blot and protein identification.** Whole body extracts from N2 or *prmt-1* mutant worms were obtained by homogenizing 20 μL of wet packed worms in 2-DE buffer (7M urea, 2M thiourea, 30 mM Tris, 4% CHAPS, 0.01% Triton X-10, 60 mM DTT) with protease inhibitor cocktail (Nacalai tesque) using sonication. After centrifugation, proteins were precipitated with methanol/chloroform and re-suspended in 2-DE buffer. Three hundred microgram of protein was separated with 75 mm pH 5–8 agarose stick gel followed by 10% SDS-PAGE gel. The resulted gels were either stained with Sypro Ruby (BioRad) fluorescent dye or transferred to PVDF membrane and

blotted with ADMA antibodies. N2 specific Western blotting spots were picked out from Sypro Ruby gel after merging the two staining results.

Detected PRMT-1 substrates were identified with MALDI-TOF/MS according to the protocol previously reported (20). Stained protein spots were excised and dehydrated with acetnitrile, and then reduced and alkylated with DTT and iodoacetamide before tryptic digestion in situ. Tryptic peptides were desalted by binding and then elution from a C18 Zip-tip (Millipore), and then mixed with α-cyano-4-hydroxycinnamic acid (Wako) matrix and spotted onto the stainless steel plate. The dried spots were analyzed by MALDI-TOF mass spectrometry (ultrafleXtreme, Bruker). The resulted peptide peaks were manually picked up, and the masses of the peptides were used for protein identification through MASCOT peptide mass fingerprint matching. The MASCOT scores larger than 57 are considered significant.

**Mitochondrial fractionation.** Worms were allowed to grow until young adult stage and harvested with M9 buffer. After clearance with sucrose flotation, worms were homogenized by using dounce homogenizer in five-time volume of mitochondria isolation buffer (MIB: 210 mM mannitol, 70 mM sucrose, 0.1 mM EDTA, 5 mM Tris, and protease inhibitor cocktail). The homogenates were centrifuged at 1,000 *g* for 10 min. The supernatants were saved, and the pellets were re-suspended in the same volume of MIB and homogenized again. After centrifuged at 1,000 *g* for 10 min, an aliquot of the

combined supernatants was saved as total lysate (TL). The rest of supernatants were centrifuged at 5,000 *g* for 10 min. The pellets were washed twice by re-suspending in 1 mL MIB and centrifuged at 2,000 *g* for 10 min. After the combined supernatants were centrifuged again at 2,000 *g* for 10 min, the heavy mitochondria (HM) were pelleted by centrifuging the supernatants at 15,000 *g* for 10 min and re-suspended in MIB. The supernatants from 5,000 *g* centrifugation were further centrifuged at 15,000 *g* for 10 min and the resulted supernatants were aliquoted as post-mitochondria supernatants (PMS). The pellets were washed by re-suspending in MIB and centrifuging at 5,000 *g* for 10 min. The light mitochondria (LM) were pelleted by centrifuging again at 15,000 *g* for 10 min and re-suspended in MIB.

The mitochondria used for *in vitro* ATP assay were isolated according to a simplified protocol as previously described (21).

**Acid hydrolysis and LC-MS/MS.** Acid hydrolysis of worm proteins was performed essentially as previously described (Kanou et al., submitted). Briefly, after mitochondrial fractionation, each fraction of worm proteins (50 mg) were hydrolyzed with 6 N HCl at 110°C for 24 hrs in glass vials. *N*-propyl-L-arginine (N-PLA, SIGMA-Aldrich) was added as the internal control.

ADMA or SDMA were quantified using a Shimadzu NexeraTM ultra high-pressure liquid chromatography system coupled to LCMS-8050TM triple quadrupole mass spectrometer (Shimadzu, Kyoto, Japan) as described

previously (Hashimoto et al. 2016). LC separation was performed on a SeQuant TM ZIC-HILIC TM column (2.1 × 150 mm, Merck KGaA, Darmstadt, Germany) with a SeQuant TM ZIC-HILIC TM Guard Fitting (1.0 × 14 mm, Merck KGaA) at 40 °C. Acetonitrile/water/formic acid (1:98:1) (A) and acetonitrile/water/formic acid (98:1:1) (B) were used as mobile phases, water-dissolved sample (1 μL) was injected and eluted with the followed gradient elution program: 95% B for 1 min, shifted to 5% in 9 min, and kept 5% for 4 min. The system was allowed to equilibrate for 7 min at 95% B prior to the next analysis. The flow rate was 0.2 mL/min.

Mass spectroscopy operating conditions were optimized as follows: interface voltage, 4.00 kV; interface current, 0.55 μV; interface temperature, 300 ˚C; desolvation line temperature, 250 ˚C; heating block temperature, 400 ˚C; drying gas (N2); 10 L / min; nebulizing gas (N2); 3 L / min; heating gas (air), 10 L / min; and collision-induced dissociation gas (argon), 230 kPa; conversion dynode potential, -10.00 kV; detector potential, -2.20 kV. Multiple reaction monitoring was used for detection of arginine derivatives with a dwell time to 100 ms. Q1 was set to transmit the parental ions MH+ at m/z 203.15 for ADMA, SDMA, and 324.6 for N-PLA. The daughter ions were monitored in Q3 at m/z 158.05, 171.95 and 70.15 for ADMA, SDMA and, N-PLA, respectively. All analyses and data processing were completed with the

LabSolutions Ver. 5.60 software (Shimadzu Scientific Instruments, Inc., Columbia, MD).

***In vitro* ATP assay.** The protein concentrations of isolated mitochondria were measured by DC protein assay (BioRad) and adjusted to 0.2 mg/mL with buffer B (225 mM sucrose, 44 mM $KH_2PO_4$, 12.5 mM Mg acetate, and 6 mM EDTA). Commercially purchased ADP (Wako) was incubated with glucose and hexokinase to deplete the residual ATP contamination before use. After reaction, the hexokinase was inactivated by heating to 99°C for 3 min. *In vitro* ATP assay was conducted in 96-well plate (Corning) with every sample measured in triplicate. Twenty microliters of different combinations of intermediate metabolites (PM: 5 mM pyruvate + 5 mM malate; SM: 25 mM succinate + 5 mM malate; GM: 50 mM glutamate + 25 mM malate; PCM: 0.25 mM palmitoyl-$_L$-carnitine + 10 mM malate) and 10 μL of 1 mM ADP were added to the wells, followed by 20 μL of isolated mitochondria or buffer B as background. The produced ATP was measured based on luciferin/luciferase reaction by ATP Bioluminescence Assay Kit HS II (Roche) under the manufactories' instructions. After 50 μL of luciferase reagent was added to the reaction, the luminescence was read by Wallac 1420 ARVOsx multilabel counter (Winpact Scientific) at different time points.

**MitoSOX staining and imaging.** Adult worms were wounded by microinjection needles to increase the permeability of MitoSOX Red molecular probe (Invitrogen). After wounding, worms were immediately transferred to MitoSOX Red staining solution (5 μM in M9, prepared from a 5 mM stock in DMSO before use) and stained in the dark with for 20 min at room temperature. Stained worms were washed three times with M9 before imaging under fluorescent microscope with DsRed filter.

**Food-avoidance assay.** Food-avoidance assay was performed as previously described (8). Briefly, one milliliter of overnight culture of RNAi *E. coli* was pelleted and re-suspended in 50 μL of LB, then dropped in the center of 3.5-cm dishes containing 1 mM IPTG. For NGM dishes, 50 μL of OP50 was seeded. Dried dishes were kept at room temperature overnight to allow the IPTG induction. Only circular lawns of uniform size and density were used for food-avoidance assays. Synchronized L1 worms (about 50 animals per dish) were dropped into the center of each bacterial lawn. Food-avoidance phenotypes were scored when the worms grow to the young adult stage.

**RNA extraction and quantitative RT-PCR.** Synchronized L1 worms were allowed to grow to L4 stage and collected. Worms were then washed with M9 buffer and re-suspended in ISOGEN (Nippon Gene). After three cycles of freeze/thaw, worms were incubated at room temperature for 5 min. Worm

debris was removed by centrifugation at 13,200 rpm for 15 min at 4°C. Total RNA was obtained by isopropanol precipitation and RQ1 RNase-free DNase (Promega) treatment. Five-hundred ng of total RNA was reverse transcribed using ReverTra ace kit (TOYOBO) and then real-time quantitative PCR reactions were performed on a Thermal Cycler Dice using a SYBR Premix Ex Taq II (TaKaRa). Relative gene expression was determined by ΔΔCT method. Primers used for amplifications were as follows:

*act-1*, the forward (5'-GGTTGCCGCTCTTGTTGTAG-3') and the reverse (5'-CTTCTGTCCCATACCGACCA-3'); *cyp-34a2*, the forward (5'-TTTGAAACATGCGCCCGCTC-3') and the reverse (5'-CGCGTCGTCCTGTTCAAACC-3'); *cyp-14a5*, the forward (5'-ACGCCTTTGTCAATCGTGCC-3') and the reverse (5'-CCTGCCCAAGCCAAAATCCC-3'); *ugt-31*, the forward (5'-TTGCGGACACACTGACCGAG-3') and the reverse (5'-CACACCGATTTCGTGCCTCC-3'); *ugt-26*, the forward (5'-AGCCCGAGGATTTCAGCTCAG-3') and the reverse (5'-TGCATCGAACAGTTTGGCGAG-3'); *gst-24*, the forward (5'-CACCCCACTACGCCAACTCA-3') and the reverse (5'-GCGCGAAGACCTCCTTTTGG-3'); *gst-29*, the forward (5'-CTCGTTGGAGATGGGCTCACA-3') and the reverse (5'-GAGCTGCCAATTTCGGGTGC-3'); *cyc-1*, the forward (5'-AGGACGGAACACCAGCAACA-3') and the reverse (5'-

GTCATGGAATGGCTCTGCGG-3'); *cco-1*, the forward (5'-AGCCTCGCCAGAAGACTACG-3') and the reverse (5'-TCTCCAGCAAGACGAGCGAG-3'); *atp-5*, the forward (5'-ACTGGTCGAAGCTCGCCGAG-3') and the reverse (5'-ACTCGGCTGGAACCTCTCCG-3').

**Mitochondria to body mass ratio.** Non-gravid young adult worms were collected and wet packed mass was measured as the body mass. Mitochondria was isolated as described above and resuspended in 100 μL of MIB. The mitochondrial protein concentrations were measured by DC protein assay to obtain the mitochondrial mass. The ratio between mitochondrial and body mass was calculated.

**Metabolome analysis.** Synchronized, arrested L1 worms were transferred to NGM plates seeded with OP50 and harvested on adult day 1 stage. The mass of wet packed worms was measured, and 30.64 mg of N2 or 47.51 mg of *prmt-1(ok2710)* were sent to Human Metabolome Technologies Co. (Japan), the metabolites were extracted by methanol/chloroform and subjected to metabolome analysis by capillary electrophoresis-time of flight mass spectrometry (CE-TOFMS). The detected 208 metabolites (110 cations and 98 anions) were clustered according to the metabolic pathways and drawn in the heatmap.

**DNA microarray.** Total RNA was prepared from N2 or *prmt-1(ok2710)* mutant worms as described above and sent to Hokkaido System Science Co Ltd. (Japan) for cDNA microarray based gene expression profiling. For data analysis, genes with the expression levels over two-fold increase in *prmt-1* (ok2710) relative to N2 were extracted and functionally classified through Database for Annotation, Visualization, and Integrated Discovery (DAVID). The enriched functional groups with *p* value less than 0.05 were considered significant. The relative expression levels of metabolism processing related genes or mitochondrial function related genes were normalized by Cluster 3.0 and plotted in heatmaps with Java TreeView.

**Statistical analysis.** Results were presented as mean ± standard error of the mean (SEM). Statistical significances were determined by two-tailed unpaired Student's t-test. Significant differences are indicated as follows: *$p < 0.05$, **$p < 0.01$, and ***$p < 0.001$.

# CHAPTER 3
# IN VIVO SUBSTRATES IDENTIFICATION OF PRMT-1 IN C. ELEGANS

## Purposes

According to previous studies (1-5), the cellular functions PRMT1 has been extensively explored based on the identification of its various *in vitro* substrates. However, it is doubtful that these *in vitro* substrates are targeted by PRMT1 *in vivo* due to the different environments for the reaction. The assembly of PRMT1 complex with other regulatory factors could largely change the bulk activity of PRMT1 or result in unbiased activity towards its preferred substrates according to the cellular environment. We suppose that the physiological roles of PRMT1 remained largely unclear at least partially due to the lack of knowledge of its *in vivo* substrates. To further explore the physiological roles of PRMT-1-mediated asymmetric arginine dimethylation, we attempted to systematically identify *in vivo* substrates of PRMT1.

## Results

As we reported previously (19), nematode *C. elegans* PRMT-1 is the predominant type I arginine methyltransferse and its null mutant, *prmt-1(ok2710)*, is viable unlike lethal phenotypes of PRMT1-deficient mouse and *Drosophila* (22, 23). We therefore employed *C. elegans* as an ideal animal model for screening *in vivo* substrates of PRMT-1 with the strategy of two-

dimensional (2-D) proteomic analysis (Figure 3-1) combining Sypro Ruby protein stain and Western blot against two distinct asymmetric dimethylarginine antibodies, ASYM24 (19, 24, 25) and ASYM26.

Since different lots of antibodies may give different performance, we tested the two ADMA antibodies used for 2-D proteomic analysis. Whole worm extracts from N2 or *prmt-1(ok2710)* were separated by one-dimensional SDS-PAGE and blotted with either ASYM24 or ASYM26 (Figure 3-2). Robust signals were detected with ASYM24 on N2 extracts, while multiple bands of low molecular weight were detected with ASYM26. Remarkably, the signals on N2 extracts greatly decreased on *prmt-1(ok2710)* sample with both antibodies. This result is in good agreement with our previous finding by high performance liquid chromatography (HPLC) (9), indicating that both antibodies are specific for ADMA-proteins.

Two-dimensional electrophoresis (2-DE) followed by Western blot against ASYM24 (Figure 3-3 upper panels) or ASYM26 (Figure 3-3 middle panels) revealed 10 spots of proteins containing ADMA in N2 sample when compared to *prmt-1(ok2710)* mutants as a negative control. Among them, spots 1, 2, 3, and 4 were detected by both antibodies, while the others were specific to either ASYM24 or ASYM26 antibody. This result appears to be due to the difference in the immunogens of the two antibodies, which in turn broadens the spectrum of proteins allowed to be detected. Next, to identify the proteins detected by Western blot, the same samples separated by 2-DE were stained with Sypro

Ruby fluorescent dye (Figure 3-3 lower panels) and then overlapped with the images of Western blot. We found that nine out of ten ADMA spots have their corresponding spots on the Sypro Ruby staining and also show no significant change in their intensity between N2 and *prmt-1(ok2710)* mutants. These data suggest that the nine spots (Table 1) are bona fide candidates of ADMA modification in *C. elegans*.

The N2 specific spots were pick out manually and digested with trypsin. The results of protein identification by MALDI-TOF/MS are shown in Table 1. The MASCOT probability scores over 57 are considered significant.

**Discussion**

Among the nine substrates identified in this study, Nuclear Hormone Receptor 12 (NHR-12) has its human version Hepatocyte Nuclear Factor 4 gamma (HNF4γ) as a known substrate of PRMT1 previously. Importantly, the methylated arginine in HNF4γ is well conserved in NHR-12 (Figure 3-4), indicating the functional significance of PRMT1-mediated methylation on this protein across different species. Although the physiological functions of another identified substrate, F41H10.3, are unknown in *C. elegans*, its homolog, MUCIN-2, a secretary protein found in the mucous membrane of intestine, is a well-characterized factor involved in the intestinal defense to enteric pathogens (47), raising the possibility that PRMT1 may play roles in the gastrointestinal mucosal barrier. It is known that RNA-binding proteins are a large group of

substrates targeted by PRMTs (5) including ribosomal proteins (5). The methylation on RPS3 by PRMT1, RPS2 by PRMT3, and RPS10 by PRMT5 have been shown to be related with ribosomal assembly or biogenesis, suggesting that the modification of RPS4 and RPL4 by PRMT-1 may play similar roles in *C. elegans*. Surprisingly, the current results of 2-D proteomic study revealed substrates with elusive subcellular localizations including endoplasmic reticulum (ER) and mitochondria, indicating asymmetric arginine dimethylation may be involved in a broad spectrum of cellular processes *in vivo*. The ER specific calcium-binding molecular chaperone CRT-1 was shown to have multiple functions in *C. elegans* such as preventing protein aggregation during heat shock or suppressing necrotic cell death, and be important for normal fertility or development. The asymmetric arginine dimethylation of CRT-1 can therefore exert regulatory effects on its functions. Notably, three mitochondrial proteins, HSP-60, ATP-2, and Y38F1A.6, were found to be potential substrates of PRMT-1 *in vivo*. Among them, HSP-60 is a mitochondria-specific chaperone which facilitates mitochondrial protein folding and is induced under mitochondrial stresses (11-13). ATP-2, the beta subunit of ATP synthase, which holds the binding and catalyzing activity of ADP and Pi, is crucial for the key steps in ATP synthesis. Y38F1A.6, the putative alcohol dehydrogenase, is involved in the metabolism of γ-hydroxybutyrate (GHB) which is an important neurotransmitter used as psychotropic drugs.

Although previously several studies reported that asymmetric arginine dimethylation was found on mitochondrial proteins also in human cells or Trypanosomes (29), the correlation between this modification and mitochondrial function has never been addressed. On the other hand, there is a growing body of evidence showing that PRMT1 is largely involved in mitochondria-related disorders such as cardiovascular diseases and neuronal degradative diseases (3, 5), while the possible mechanisms remain largely unknown. Therefore, the identification of the three proteins prompted us to further investigate the functional significance of this modification in mitochondria.

Figure 3-1

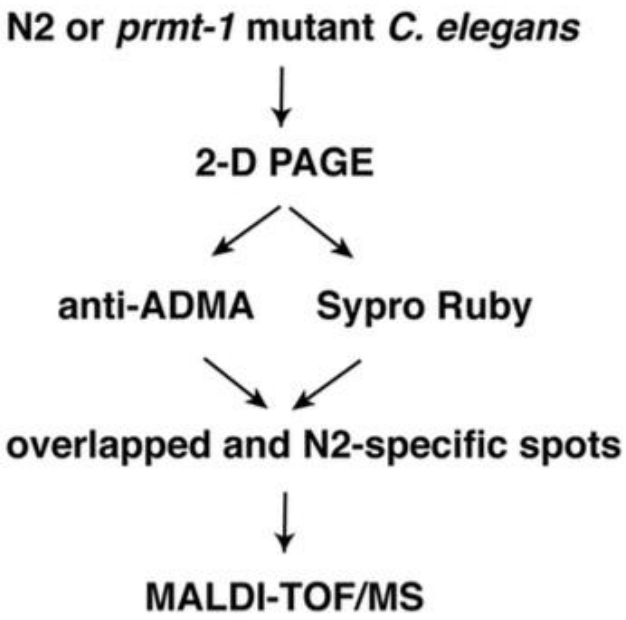


Figure 3-1. Schematic workflow of two-dimensional (2-D) Western blot for identification of PRMT-1 substrate in *C. elegans*. Briefly, whole cell extracts from wild-type N2 or *prmt-1(ok2710)* mutants were subjected to 2-D PAGE and blotted with anti-ADMA antibodies. N2-specific spots were picked out from Sypro Ruby stained gels and identified by MALDI-TOF/MS.

Figure 3-2

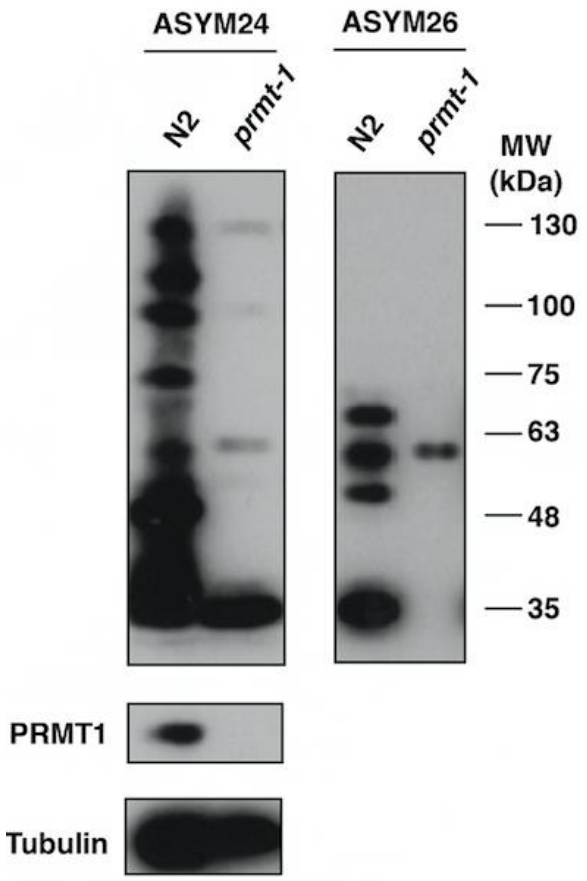


Figure 3-2. The two kinds of antibodies used in this study detected protein-ADMA. Whole protein lysate from N2 or prmt-1 worms were blotted with ASYM24, ASYM26, PRMT-1, or Tubulin antibodies.

Figure 3-3

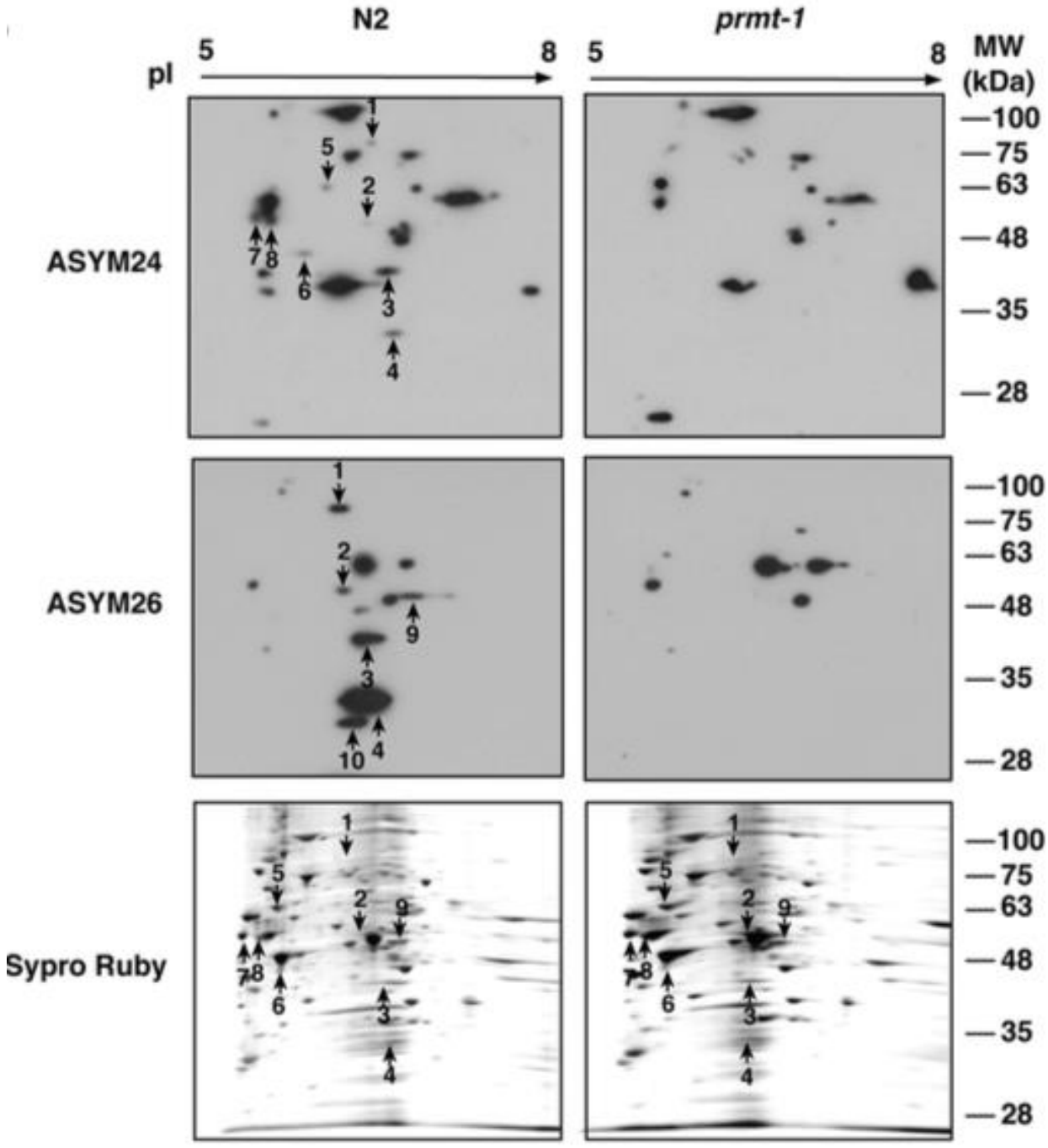


(legend on the next page)

Figure 3-3. Whole cell extracts from N2 or *prmt-1(ok2710)* mutants on adult day 1 were separated by 2-D PAGE, followed by Western blotting with ASYM24 (upper panels) or ASYM26 (middle panels) antibodies. After merging with Sypro Ruby stained gels (lower panels), N2-specific spots detected with anti-ADMA antibodies (indicated by arrows and numbers) were manually picked out for MALDI-TOF/MS analysis.

Table 1

**Protein identification of major *C. elegans* PRMT-1 substrates**

| Spot No. | Protein Identification | Homolog | Fragment Coverage (%) | MASCOT Probability Score | UniProtKB Entry | Protein Mass (kDa) | Subcellular Localization |
|---|---|---|---|---|---|---|---|
| 1 | F41H10.3, isoform d | Mucin-2 | 35 | 59 | V6CLM1 | 86 | Exc |
| 2 | NHR-12, isoform c | HNF4γ | 41 | 60 | I2HAH0 | 52 | Nu |
| 3 | RPL-4 | RPL4 | 66 | 100 | O02056 | 39 | Rb |
| 4 | RPS-4 | RPS4X | 72 | 94 | Q9N3X2 | 29 | Rb |
| 5 | HSP-60 | HSPD1 | 53 | 88 | P50140 | 60 | Mt |
| 6 | ACT-4, isoform c | ACTB | 61 | 105 | Q6A8K1 | 40 | Cy |
| 7 | CRT-1 | CALR | 58 | 121 | P27798 | 46 | ER |
| 8 | ATP-2 | ATP5B | 43 | 157 | P46561 | 58 | Mt |
| 9 | Y38F1A.6 | HOT | 55 | 75 | Q9U2M4 | 51 | Mt |

(legend on the next page)

Table 1. PRMT-1 substrate proteins revealed by 2-D WB were identified by mass spectrometry analysis of tryptic fragments from gel spots. Tryptic fragment coverage from MALDI-TOF/MS of the identified proteins is showed, from which a MASCOT probability score was generated. Probability score over 57 was considered as a significant match ($p < 0.05$). In addition, the UniProtKB entry, estimated protein mass, subcellular localization, and ortholog of the identified proteins are included.

# CHAPTER 4
# A MAJOR CONTRIBUTION OF PRMT-1 TO ASYMMETRIC ARGININE DIMETHYLATION OF MITOCHONDRIAL PROTEINS

## Purposes

In chapter 3, by taking advantage of the fact that *prmt-1* is the only type I PRMT and its deficient mutant is alive in *C. elegans*, we performed 2-D Western blot based proteomic analysis with two distinct ADMA antibodies and identified 9 *in vivo* substrates of PRMT-1 by MALDI-TOF/MS. Direct interaction between the target proteins and the enzyme is usually a convincing evidence for the enzymatic reactions to occur. To confirm the potential of the three mitochondrial proteins being methylated by PRMT-1, it is necessary to examine the methylation signal by using purified proteins and distinct detecting method other than antibody under *in vitro* conditions.

Furthermore, to assess the contribution of PRMT-1 to the formation of asymmetric arginine dimethylation on mitochondrial proteins, the mitochondria from N2 or *prmt-1* mutant worms are to be isolated and subjected to protein-ADMA quantification.

## Results

To confirm the potential of the three mitochondrial proteins being substrates of PRMT-1, we performed GST pull-down and *in vitro* methylation assays by using FLAG-tagged PRMT-1 purified from HEK293T cell extracts together with GST-fused recombinant proteins. As shown in Figure 4-1, PRMT-1 bound to the three mitochondrial proteins *in vitro,* supporting the possibility that they could be substrates of PRMT-1. Actually, we found that HSP-60 is methylated as well as the forkhead domain of DAF-16, a positive control (19), and the other two mitochondrial proteins ATP-2 and Y38F1A.6 are also methylated, albeit at a lower extent than HSP-60 (Figure 4-2).

Next, to investigate the contribution of PRMT-1 to asymmetric arginine dimethylation of total mitochondrial protein *in vivo*, we performed subcellular fractionation of mitochondria from *C. elegans* and quantified the amounts of ADMA in proteins by using LC-MS/MS. Efficient isolation of light and heavy mitochondria from total extracts of wild-type and *prmt-1(ok2710)* mutants were verified by Western blot with organelle markers (Figure 4-3). Notably, LC-MS/MS analysis demonstrated that *prmt-1(ok2710)* mutants has extremely low levels of ADMA in both mitochondrial fractions compared with that of N2 (Figure 4-4). In contrast, levels of symmetric dimethylarginine (SDMA) were increased in light but not heavy mitochondrial fraction (Figure 4-4), which is partially consistent with previous observations in mouse models (17, 26). Taken together, these results indicate that PRMT-1 serves as the major enzyme

catalyzing asymmetric arginine dimethylation in mitochondria, and the loss of PRMT-1 alters the dynamics of SDMA formation especially in light mitochondrial fraction.

**Discussion**

*In vitro* experiments showing that the three mitochondrial proteins interact and are methylated by PRMT-1, partially confirmed the results of the 2-D proteomic analysis based *in vivo* substrate identification (Chapter 3). However, since the *in vivo* reaction context can be largely different from *in vitro*, we have scheduled to confirm the *in vivo* methylation of the three mitochondrial proteins. The modified arginine sites will be identified by MALDI-TOF/MS/MS either from the corresponding spots on 2-D result or from the immunoprecipitated protein with specific antibodies. This information is important for the following functional study of asymmetric arginine dimethylation on the three mitochondrial proteins by mutagenesis.

In consistence with our previous finding that PRMT-1 is the predominant type I PRMT in *C. elegans*, mitochondrial fractionation from either N2 or *prmt-1* mutant worms showed that PRMT-1 contributes to almost all the asymmetric arginine dimethylation formation on mitochondrial proteins as revealed by acidic hydrolysis followed by LC-MS/MS analysis. Intriguingly, Western blot results showed that PRMT-1 itself is not localized in mitochondria, which is in line with the previous knowledge that PRMT-1 is mainly localized in nucleus

and cytoplasm (5). Therefore, we hypothesize that PRMT-1 methylates the mitochondrial proteins in the cytoplasm before they translocalize into mitochondria. This would make the asymmetric arginine dimethylation different from the other post-translational modifications on mitochondrial proteins, such as phosphorylation and acetylation, which either are mediated by mitochondrial enzymes or occur spontaneously (19, 20). The modification of mitochondrial proteins in cytoplasm is supposed to provide extra regulations on mitochondrial functions including mitochondrial protein import, although the protein level of ATP-2 in mitochondrial fractions doesn't seem to be altered by *prmt-1* depletion (Figure 4-3). However, whether PRMT-1 methylates its mitochondrial substrates directly *in vivo* needs to be further examined.

Figure 4-1

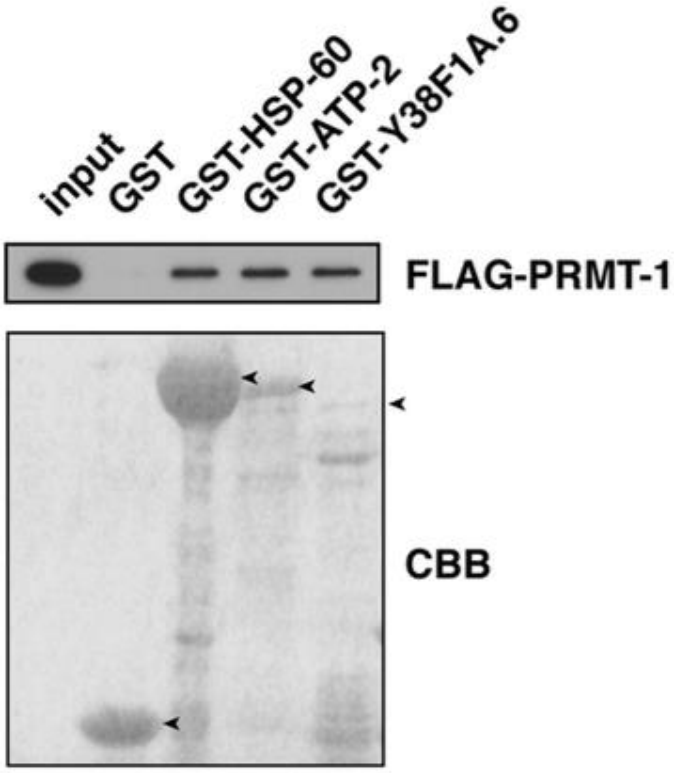


Figure 4-1. HSP-60, ATP-2, and Y38F1A.6 bind to PRMT-1 *in vitro*. GST pull-down assay was performed with FLAG-PRMT-1 and GST, GST-HSP-60, GST-ATP-2, or GST-Y38F1A.6, followed by Western blotting (upper panel) and CBB staining (lower panel). Arrowheads indicate the position of GST proteins.

Figure 4-2

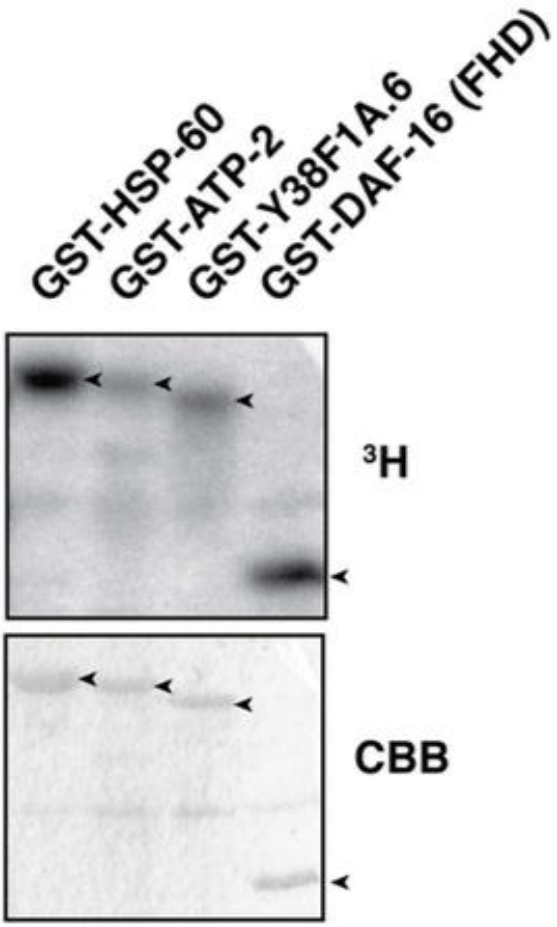


Figure 4-2. PRMT-1 methylates HSP-60, ATP-2, and Y38F1A.6 *in vitro*. FLAG-PRMT-1 was incubated with GST-HSP-60, GST-ATP-2, GST-Y38F1A.6, or GST-DAF-16 (FHD) in the presence of [$^{3}$H]SAM. Arrowheads indicate the position of GST proteins in CBB staining (lower panel) and their corresponding autoradiography bands (upper panel). FHD, forkhead domain.

Figure 4-3

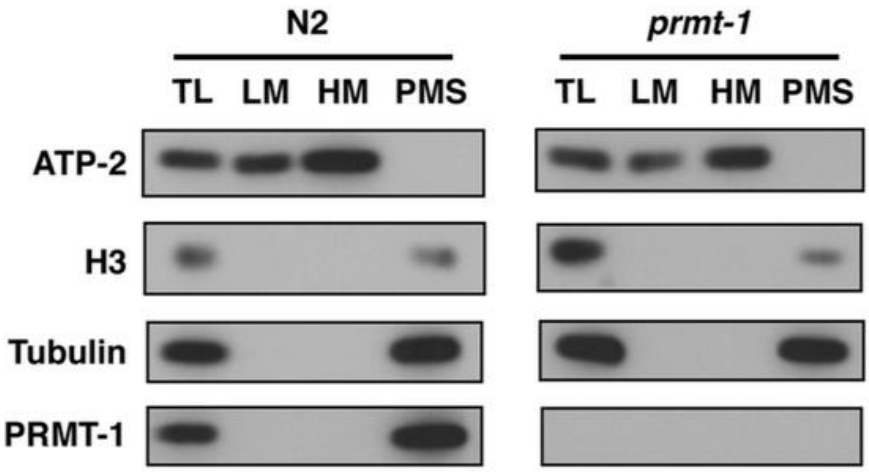


Figure 4-3. Mitochondrial fractionation of whole cell extracts from N2 or *prmt-1(ok2710)* mutants. Each fraction was blotted with antibodies against ATP-2 (mitochondrial marker), H3 (nuclear marker), Tubulin (cytoplasmic marker), or PRMT-1. TL, total lysate; LM, light mitochondria; HM, heavy mitochondria; PMS, post-mitochondria supernatant.

Figure 4-4

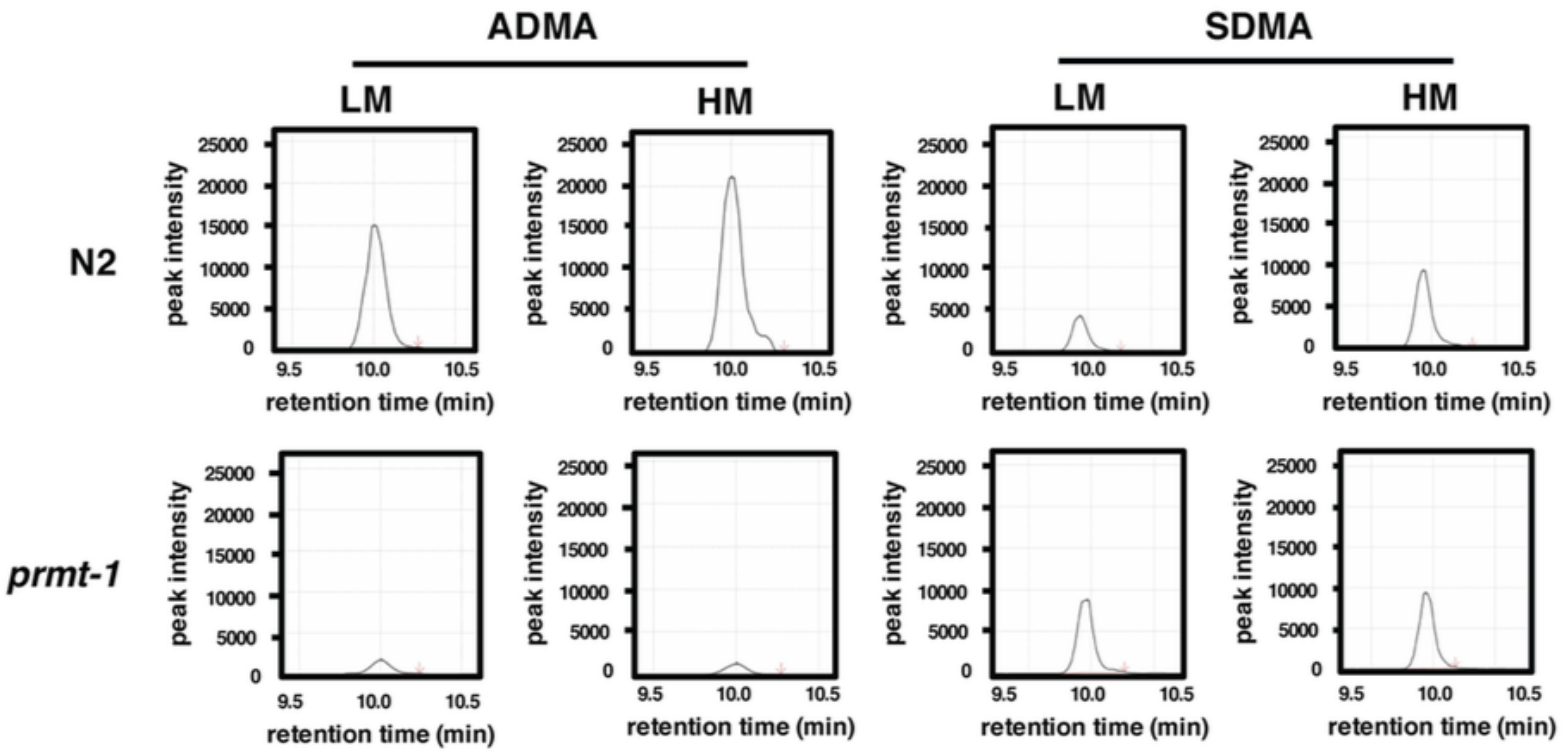


Figure 4-3. Determination of ADMA and SDMA levels in mitochondrial fractions. Fifty micrograms of light or heavy mitochondrial proteins from N2 or *prmt-1(ok2710)* mutants were subjected to acidic hydrolysis and then analyzed with LC-MS/MS.

# CHAPTER 5
# IMPAIRED ATP SYNTHESIS IN MITOCHONDRIA FROM PRMT-1-NULL MUTANTS

## Purposes

Mitochondria plays central roles in cellular metabolism. While post-translational modifications such as phosphorylation and acetylation/deacetylation have been shown to closely related to the functions of mitochondria (19, 20), the roles of arginine methylation on mitochondrial metabolism remains largely unclear. According to the results of Chapter 3 and 4, asymmetric arginine diemthylation was found on mitochondrial proteins and PRMT-1 contributes to almost all the formation of asymmetric arginine dimethylation in isolated mitochondria from *C. elegans*. We next asked if the bulk asymmetric arginine methylation on mitochondrial proteins is involved in mitochondrial functions.

## Results

It has been shown that mammalian PRMT1 facilitates mitochondrial biogenesis through methylation of peroxisome proliferator-activated receptor-γ coactivator 1α (PGC1α) (27). In *C. elegans*, however, we did not observe a significant reduction in either mitochondrial mass or mRNA levels of mitochondrial genes including *cyc-1*, *cco-1* and *atp-5* in *prmt-1* mutant (Figure

5-1). A plausible explanation for this difference may be that PGC1α is not conserved in *C. elegans*. Next, since mitochondria plays central roles in cellular metabolism, we assessed the metabolites of N2 and *prmt-1(ok2710)* mutants using the CE-TOFMS-based metabolomics analysis. Based on a comparison of the identified 208 metabolites shown in a heatmap, we revealed that a global metabolic suppression occurs in *prmt-1(ok2710)* mutants (Figure 5-2A). In particular, the levels of ATP and GSH (glutathione) were decreased in *prmt-1(ok2710)* mutants (Figure 5-2B and C, respectively). These data prompted us to hypothesize that *prmt-1*-null mutation may compromise the general functions of mitochondria, presumably due to a loss of asymmetric arginine dimethylation on a large number of mitochondrial proteins.

To investigate the functional significance of asymmetric arginine dimethylation in mitochondria, we attempted to assess ATP synthesis activity using isolated mitochondria fractions. The same amounts of mitochondria fraction were prepared from N2 and *prmt-1(ok2710)* mutants and then subjected to *in vitro* ATP assay (Figure 5-3) with supply of intermediate metabolites including pyruvate, succinate, glutamate, and palmitoyl-carnitine, as substrates (Figure 5-4). Compared with the N2 control, mitochondria from *prmt-1(ok2710)* mutants exhibited a decrease in ATP production even when any substrate is supplied and at any time-course (Figure 5-5A-D).

## Discussion

As shown by the results of metabolome analysis, a global suppression of energy metabolism, including glycolytic and mitochondrial metabolism, is observed in *prmt-1* mutant worms. Since the decreased TCA cycle or oxidative phosphorylation (OXPHOS) metabolites could be resulted from the compromised glycolysis, we employed the *in vitro* ATP assay with isolated mitochondria to directly assess the mitochondrial function under the same amount of energy source input and ADP. The combination of pyruvate and malate is widely used to assess the function of TCA cycle and OXPHOS, while glutamate or succinate with malate is specific to providing electrons through complex I or II, respectively. Palmitoyl-L-carnitine, an important intermediate of fatty acid metabolism, donates the electrons through the electron transfer flavoprotein. Given that each substrate should donate electrons to the electron transfer chain via different routes but were all converted to ATP through OXPHOS, our data imply that the decreased ATP production of *prmt-1(ok2710)* mutants may be attributed to the defects in OXPHOS, especially the process from the complex III, likely due to the loss of asymmetric arginine dimethylation on OXPHOS component proteins.

Notably, ATP-2, which is the beta subunit of the ATP synthase and functions in the final step of OXPHOS, is identified as an *in vivo* substrate of PRMT-1. It would be important to examine if the loss of asymmetric arginine dimethyaltion on ATP-2 contributes to the defects of OXPHOS resulted from

*prmt-1* depletion. Previously ATP5B was reported to be phosphorylated, or acetylated. However, the functional relevance of these modifications was unknown, suggesting the potential obstacles in doing functional study of modifications on this protein probably because it's deeply buried in the inner membrane of mitochondria and only functions when assemblies into the complex of ATP synthase. Additionally, because the experimental complexity of introducing point-mutated protein into *C. elegans* (usually it takes more than three months to generate the transgenic animal), we are planning to assess the above issue in more suitable system in future study, such as in mammalian cells.

Figure 5-1

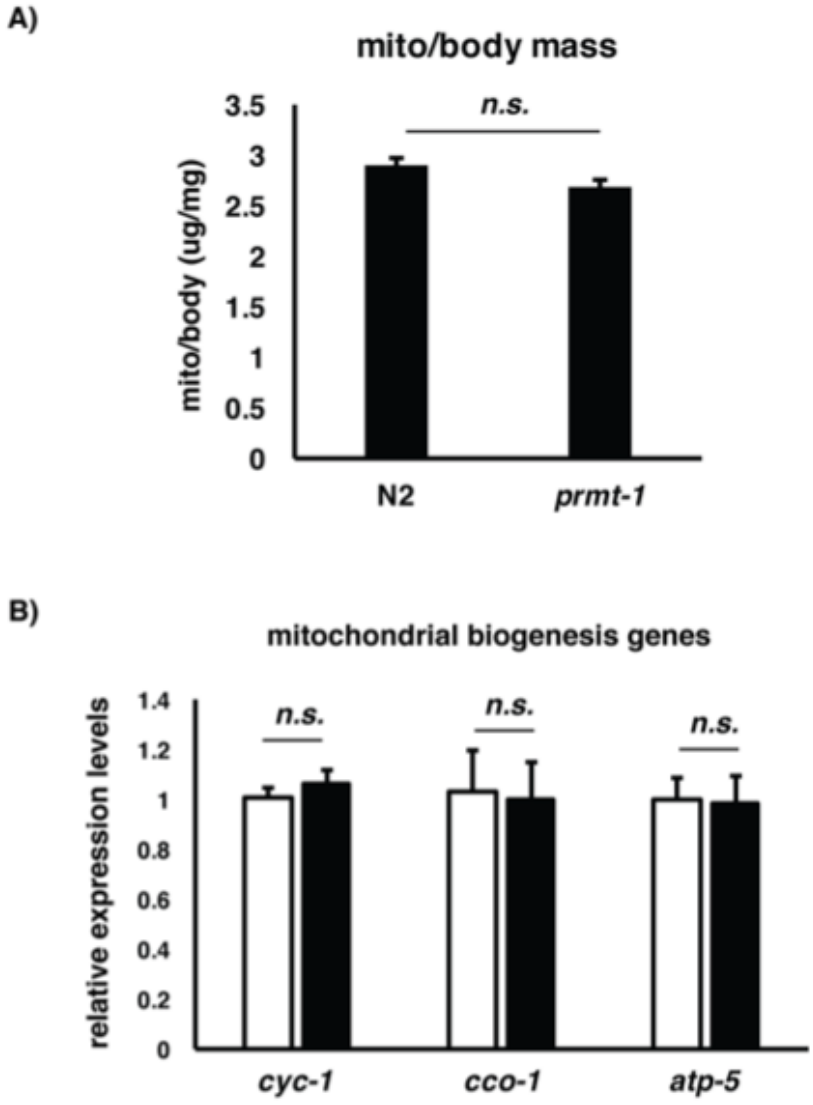


(legend on the next page)

Figure 5-1. (A) No significant decrease in mitochondria/body mass ratio was observed in *prmt-1(ok2710)* mutants. Mitochondria mass was obtained by calculating from the protein concentration and total volume of the isolated mitochondria. The wet-packed worms before mitochondrial fractionation was measured for body mass. (B) There was no difference in the expression levels of mitochondrial biogenesis genes between N2 (open bar) and *prmt-1(ok2710)* mutants (filled bar). qPT-PCR analysis was performed with total RNA from N2 or *prmt-1(ok2710)* mutants. All genes were normalized to *act-1* levels. Error bars indicate ± SEM of three independent experiments. *n.s.*: $p > 0.05$.

Figure 5-2

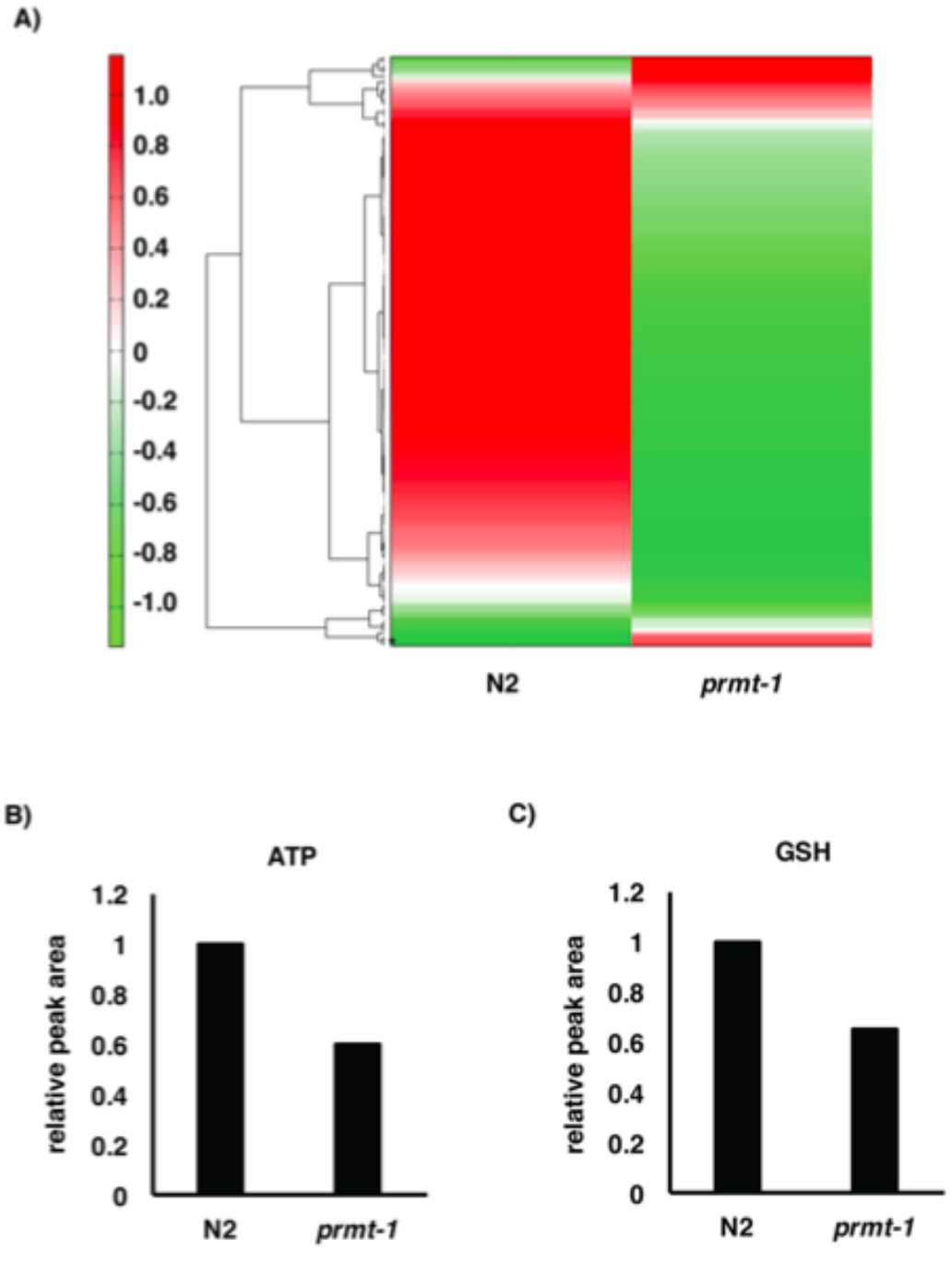


(legend on the next page)

Figure 5-2. (A) Metabolomics analysis showed a global metabolic suppression in *prmt-1(ok2710)* mutants. Metabolites from N2 or *prmt-1(ok2710)* mutants on adult day 1 were prepared and then subjected to the CE-MS-based metabolomics analysis (Human Metabolome Technologies, Inc.). The identified 208 metabolites are clustered and shown in a heatmap. (B and C) The levels of ATP and GSH were decreased in *prmt-1(ok2710)* mutants. The relative peak area was obtained from the metabolome analysis results.

Figure 5-3

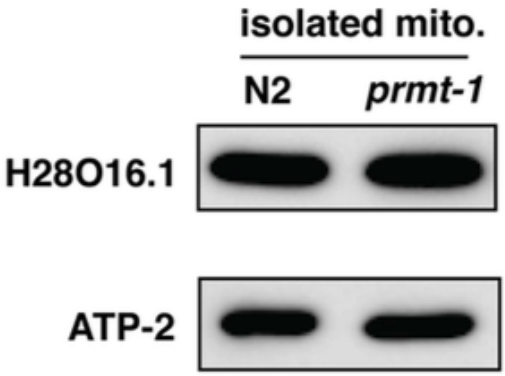


Figure 5-3. The isolation of mitochondria fractions for *in vitro* ATP assay. Isolated mitochondria fractions from N2 or *prmt-1(ok2710)* mutants were blotted with anti-H28O16.1 (ATP synthase alpha subunit) or anti-ATP-2 antibodies.

Figure 5-4

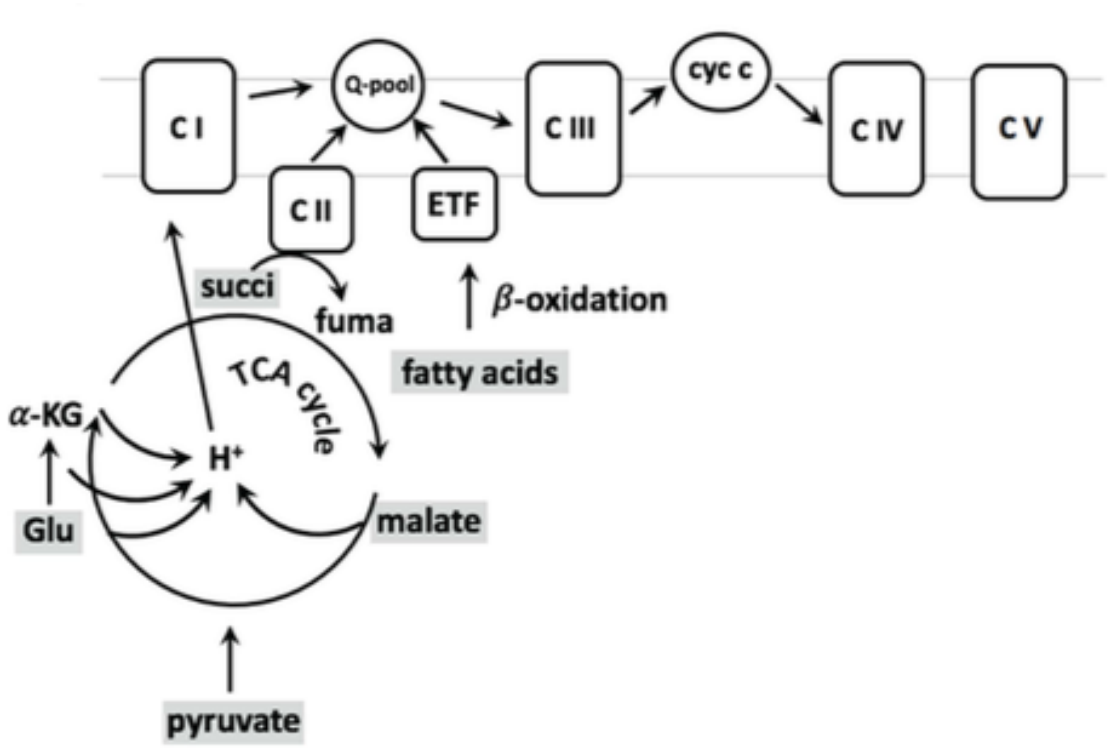


Figure 5-4. The supply of different substrates couples to oxidative phosphorylation. The substrates used in *in vitro* ATP assays are highlighted with grey background. Glu, glutamate; succi, succinate; α-KG, α-ketoglutarate; fuma, fumarate; C I-V, complex I-V; ETF, electron transfer flavoprotein; cyc c,

Figure 5-5

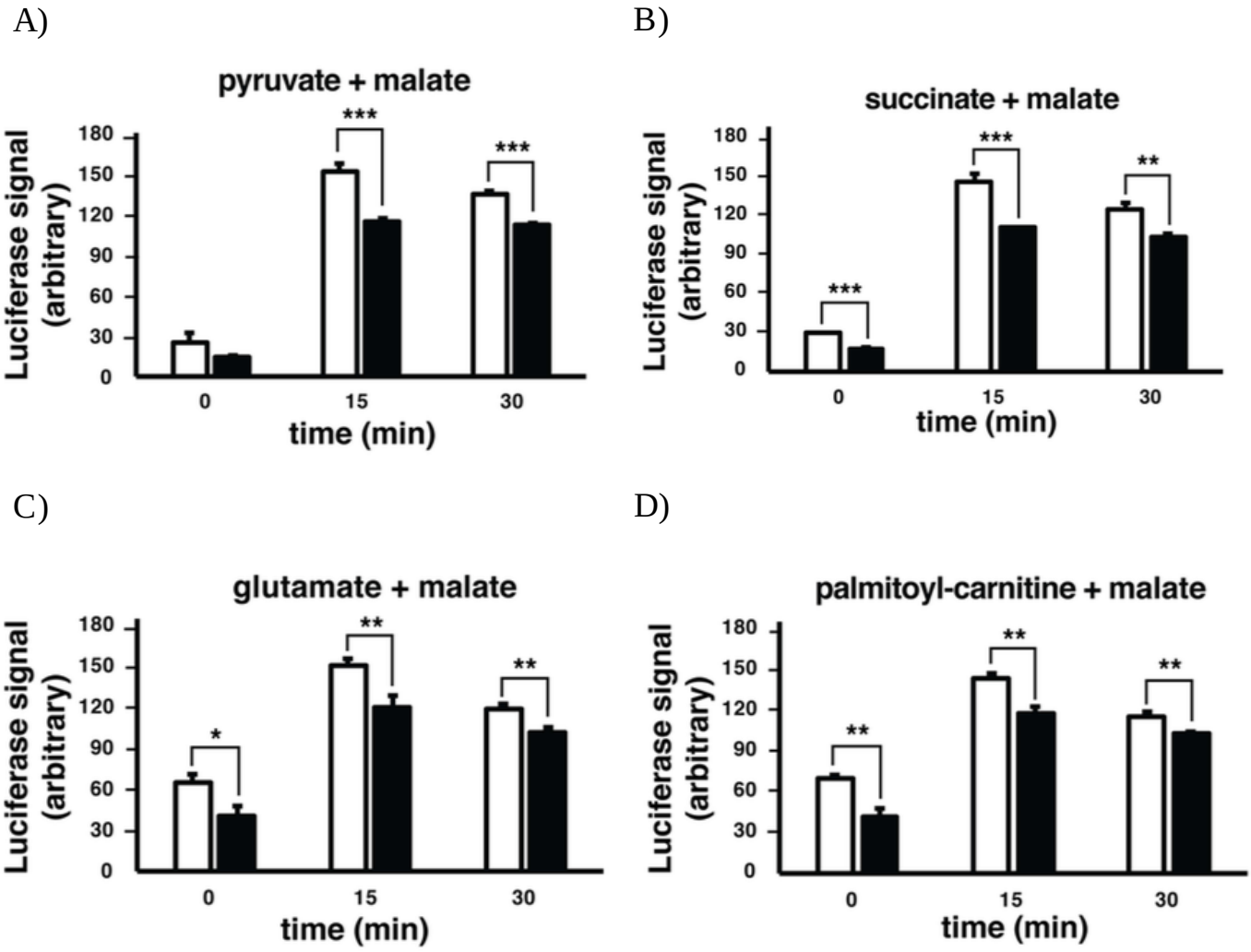


Figure 5-5. A-D, ATP synthesis of isolated mitochondria is compromised in *prmt-1*-null mutants (filled bar) compared to N2 (open bar). Different combinations of substrates were supplied and ATP synthesis was measured by *in vitro* ATP assay. Three independent experiments were performed and the representative results are showed. Error bars indicate ± SEM of triplicated measurements. * $p < 0.05$, ** $p < 0.01$, *** $p < 0.001$.

# CHAPTER 6
# INCREASED MITOCHONDRIAL ROS PRODUCTION AND MITOCHONDRIAL STRESS RESPONSES IN PRMT-1-NULL MUTANTS

## Purposes

The isolated mitochondria from *prmt-1* mutant worms exhibited decreased ATP synthesis ability when supplied with different electron donors *in vitro*, indicating possible defects in OXPHOS function. In this chapter, we are aiming to seek for biological outcomes as the evidence of impaired OXPHOS. Mitochondria is the major source of cellular ROS production, and any perturbations that cause the drop of potential across the inner membrane likely increase the mitochondrial ROS generation. Since cells use glutathione (GSH) to reduce the oxidized macromolecules by high level of ROS, it is expected to observe the up-regulation of the response against oxidative stress and a decrease in cellular GSH level. On the other hand, loss of asymmetric arginine dimethylation on mitochondrial proteins could probably obstruct their proper folding, and the suboptimal folding could either cause the malfunction of the proteins or even the unfolded protein stress in mitochondria. Therefore, we also intended to examine the mitochondria-specific unfolded protein response ($UPR^{mt}$) for the role of asymmetric arginine methylation on mitochondrial proteins in terms of protein folding.

**Results**

Abnormal OXPHOS often couples with the decreased mitochondrial membrane potential and subsequent electron leak, which in turn leads to reactive oxygen species (ROS) production (28–30). To ascertain whether *prmt-1(ok2710)* mutants increase the ROS production in mitochondria, we used the mitochondrial superoxide indicator MitoSOX for *in vivo* imaging. As shown in Figure 6-1, mitochondrial ROS was selectively detected in *prmt-1(ok2710)* mutants. Importantly, the *prmt-1* revertant strain that fully restores the amount of ADMA (19) exhibited an elimination of mitochondrial ROS, whereas another revertant strain harboring an enzymatically-inactive *prmt-1G70A* failed to attenuate the increase of ROS production in the *prmt-1* null allele. In contrast to PRMT-1, depletion of PRMT-5, the predominant type II arginine methyltransferse in *C. elegans* (Kanou *et. al*, submitted for publication), had no effect on mitochondrial ROS levels (Figure 6-2). Considering the results of *in vitro* ATP assay (Figure 5-5), these findings suggest that asymmetric arginine dimethylation by PRMT-1 contributes to normal OXPHOS in *C. elegans*.

Next, we further examined whether the impairment of mitochondrial function triggered by ablation of *prmt-1* could result in mitochondrial stress. Quantitative RT-PCR demonstrated elevation of a wide range of the mitochondrial stress response genes including oxidative stress, xenobiotic-detoxification, and pathogen-response pathway in *prmt-1(ok2710)* mutants (Figure 6-3). In addition, gene ontology analysis of DNA microarray of N2 and

*prmt-1(ok2710)* mutants revealed a global up-regulation of genes, especially those associated with metabolic processes and mitochondrial functions (Figure 6-4), suggesting that *prmt-1*-null mutants exhibit the adaptive responses to mitochondrial dysfunction.

Mitochondrial unfolded protein response ($UPR^{mt}$) is an evolutionarily conserved system that confers resistance to mitochondrial stresses by up-regulating mitochondria-specific chaperones, such as HSP-6 or HSP-60 (8, 31). To investigate whether loss of asymmetric arginine dimethylation in mitochondrial proteins could elicit the $UPR^{mt}$, we employed a highly sensitive reporter strain *zcIS13[Phsp6::gfp]* that induces *hsp-6* promoter-driven GFP expression specifically responding to mitochondrial stresses (8, 32). As shown in Figure 6-5A, knockdown of *prmt-1* led to an restricted induction of GFP in the head and tail compared with control knockdown. The activation of the *hsp-6* promoter by *prmt-1* knockdown was confirmed by Western blot with GFP antibody (Figure 6-5B). Together with a marked decrease in GSH level (Figure 5-2C), these observations clearly show that loss of PRMT-1 induces mitochondrial stress, perhaps as a result of disruption of redox homeostasis in *C. elegans*.

## Discussion

As revealed by the results of MitoSOX staining, *prmt-1* mutant worms exhibited increased level of mitochondrial ROS generation. Since the ROS elevation was rescued by the *prmt-1* wild-type but not enzymatically-deficient transgenic revertants, we suppose that the increased ROS generation was due to the loss of asymmetric arginine dimethylation on mitochondrial proteins which is necessary for the normal function of OXPHOS.

Compared to the positive control *isp-1*, the induction of mitochondrial UPR$^{mt}$ indicated by *hsp6p::gfp* was relatively weak that GFP only observed in the pharynx and the end of intestine of *prmt-1* KD while in the whole intestine of *isp-1* KD (data not shown). Although it may be due to a problem of the incomplete deletion of *prmt-1* by knockdown (we were unable to examine the activation of UPR$^{mt}$ by using the *hsp6p::gfp* reporter line in *prmt-1* mutant worms since the transgenic gene is on the same chromosome with *prmt-1* gene and this makes it difficult to introduce the *hsp6p::gfp* gene into the *prmt-1* mutant background by mating), the weak GFP induction suggested a mild mitochondrial stress when *prmt-1* is depleted. On the other hand, asymmetric arginine dimethylation could occur on a broad spectrum of mitochondrial proteins as shown by the study in Trypanosome (29). Although the complete depletion of crucial mitochondrial proteins including ATP-2 or HSP-60 causes the activation of UPR$^{mt}$ in *C. elegans*, it is highly possible that the mild

mitochondrial stress in *prmt-1* depleted worms is an integrated result of the loss of asymmetric arginine methylation on global mitochondrial proteins.

Whether the activation of UPR$^{mt}$ was related to the elevated mitochondrial ROS remains an interesting issue to be addressed. Currently we are trying to examine the level of UPR$^{mt}$ when mitochondrial ROS is blocked by antioxidant such as N-acetyl-cysteine (NAC).

Figure 6-1

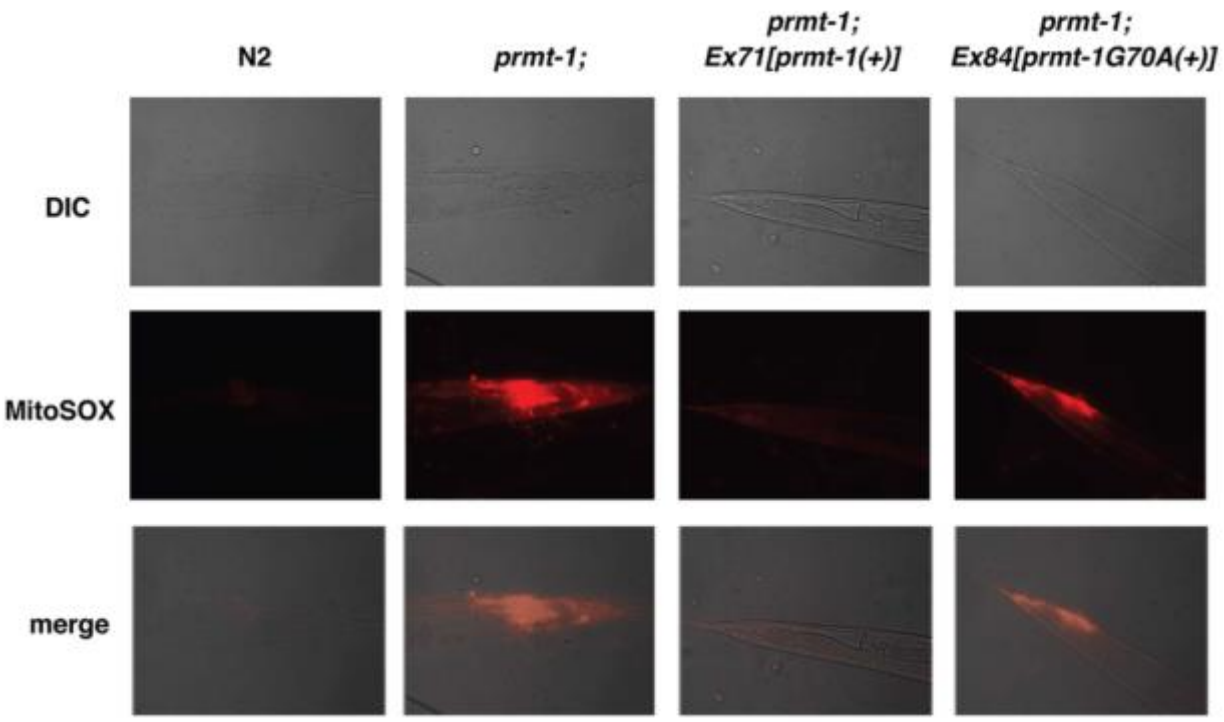


Figure 6-1. N2, *prmt-1(ok2710)*, *Ex71[prmt-1(+)];prmt-1(ok2710), or Ex84[prmt-1G70A(+)];prmt-1(ok2710)* on adult day 1 was stained with the mitochondrial superoxide indicator MitoSOX and observed with a fluorescent microscope. Representative microscopy images (original magnification 400×) are shown. DIC, different interference contrast.

Figure 6-2

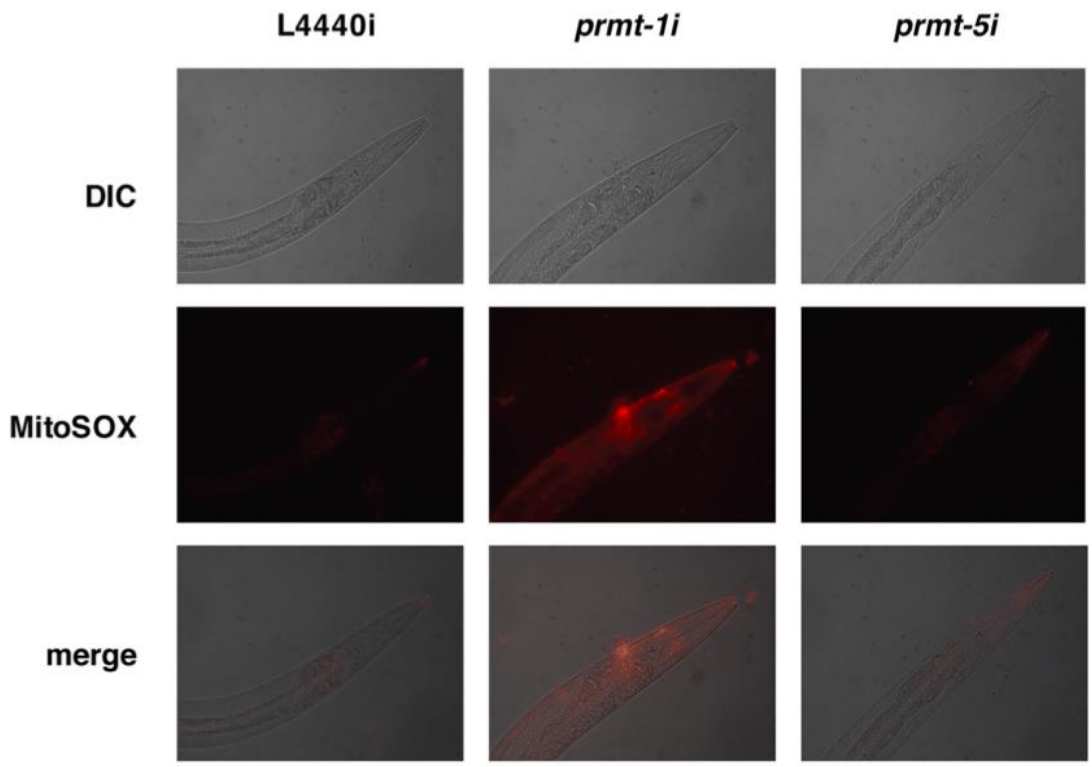


Figure 6-2. Feeding RNAi was carried out with control L4440, *prmt-1*, or *prmt-5* RNAi vectors from L4 stage. The F1 generation on adult day 1 was stained with the mitochondrial superoxide indicator MitoSOX. Representative microscopy images (original magnification 400×) are shown. DIC, different interference contrast.

Figure 6-3

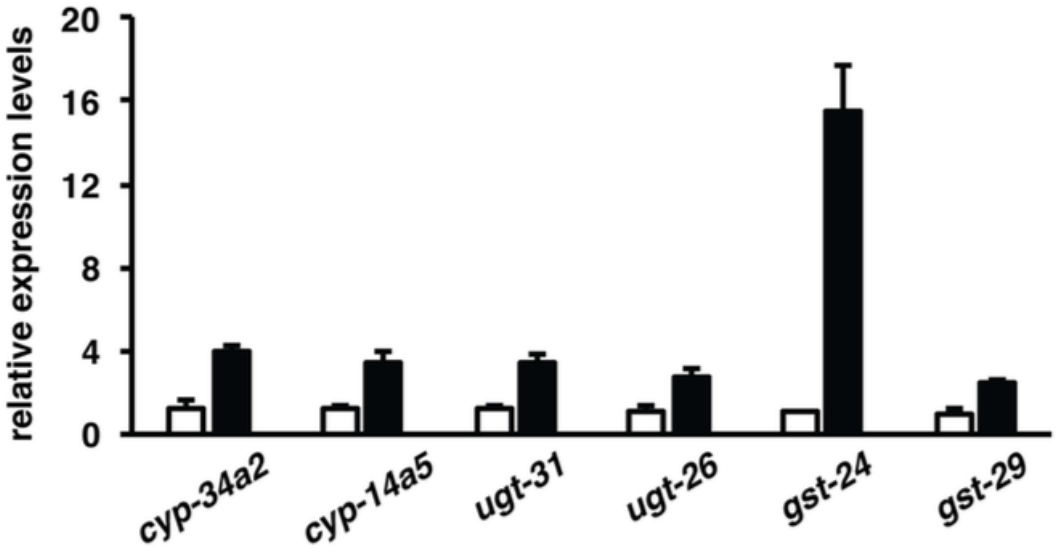


Figure 6-3. *prmt-1*-null mutants (filled bar) show elevated expression of genes involved in oxidative-stress-response, xenobiotic-detoxification, and pathogen-response pathways relative to N2 (open bar). qPT-PCR analysis was performed with total RNA from N2 or *prmt-1(ok2710)* mutants. All genes were normalized to *act-1* levels. Error bars indicate ± SEM of two independent experiments.

Figure 6-4

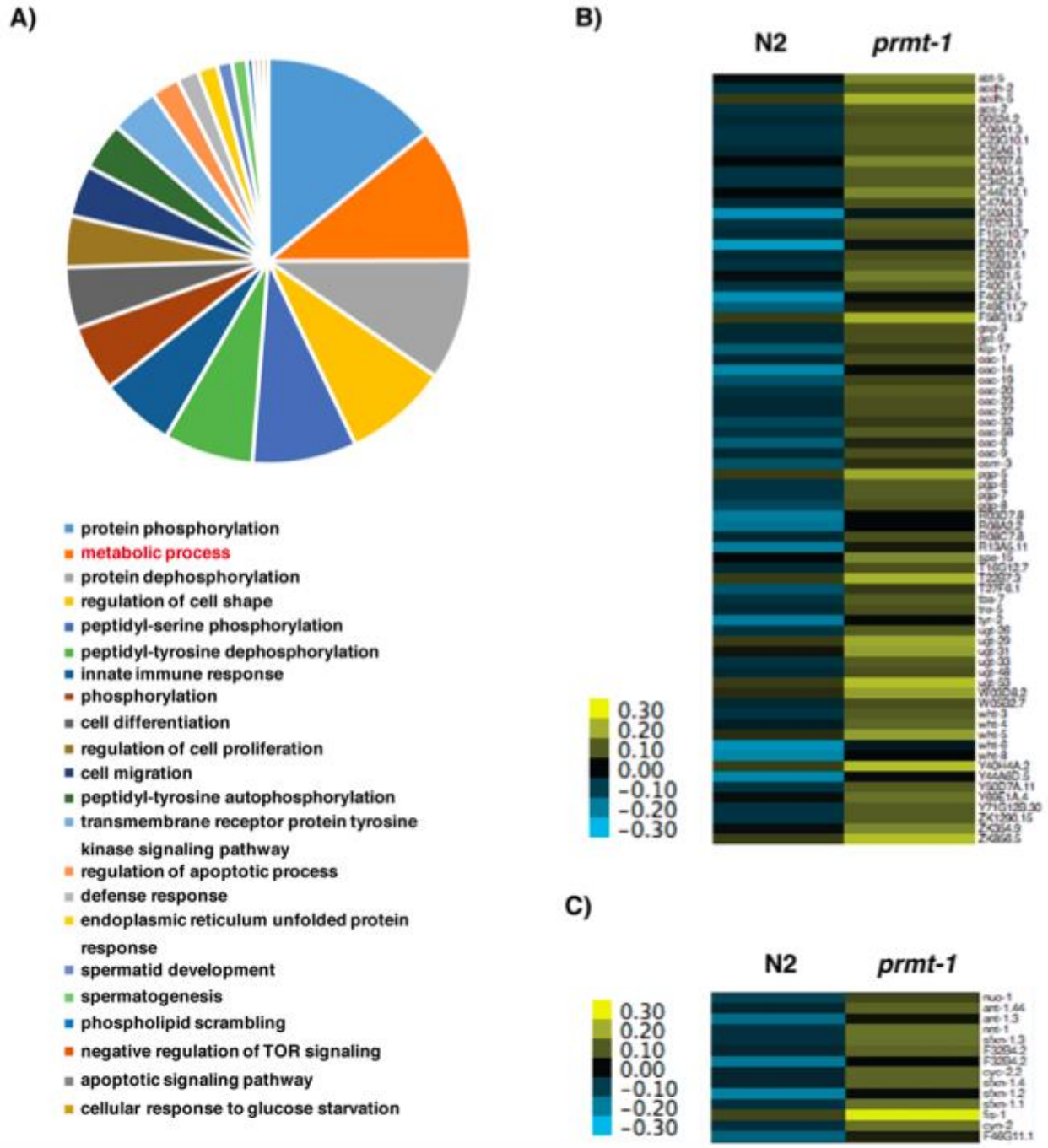


(legend on the next page)

Figure 6-4. (A) Genes related to metabolic process were enriched from total up-regulated genes in *prmt-1(ok2710)* mutants. Over 2-fold up-regulated genes identified by DNA microarray were functionally categorized through the Database for Annotation, Visualization, and Integrated Discovery (DAVID). Enrichment *p* value less than 0.05 was shown. (B and C) Seventy-four genes related to metabolic process and fourteen genes related to mitochondrial function were up-regulated in *prmt-1(ok2710)* mutants. Over 2-fold up-regulated genes were categorized through DAVID according to gene functions or cellular compartments. Metabolic and mitochondrial genes were shown by two heatmaps (B) and (C), respectively.

Figure 6-5

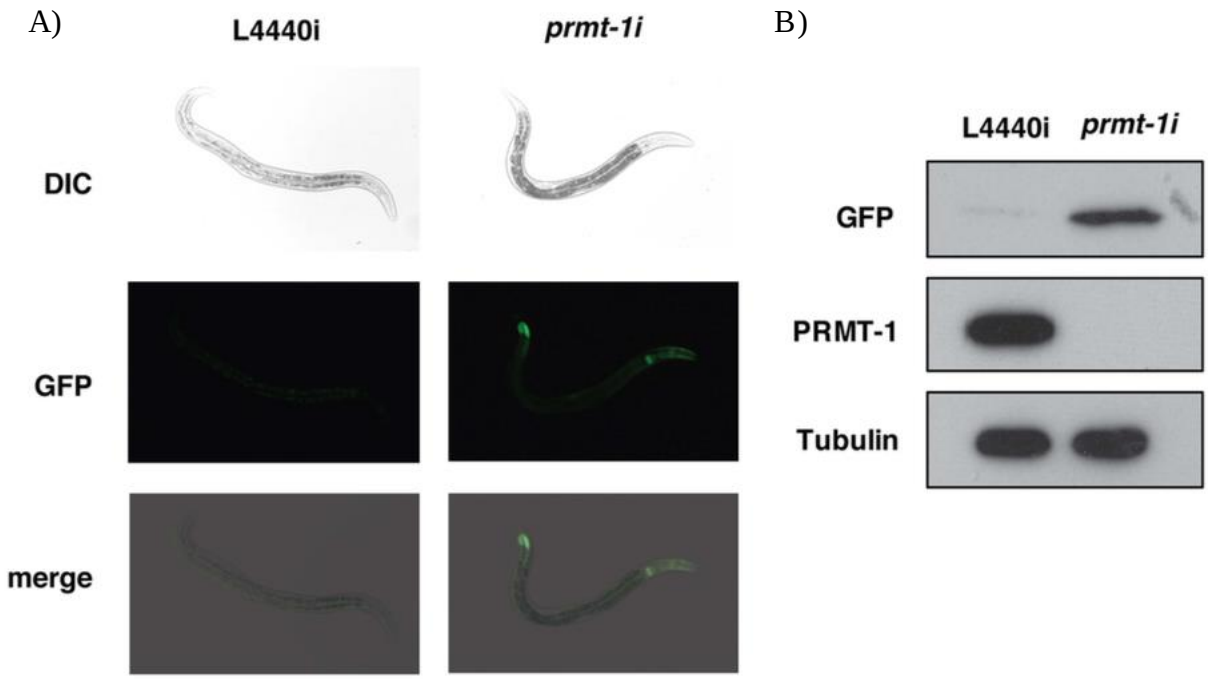


Figure 6-5. Knockdown of *prmt-1* induces GFP expression in the mitochondrial stress reporter strain *zcIS13[Phsp6::gfp]*. Feeding RNAi was carried out with control L4440 or *prmt-1* RNAi vectors from L4 stage. GFP expression was observed in the F1 generation with a fluorescent microscope (A) and Western blot with anti-GFP antibody (B). DIC, different interference contrast.

# CHAPTER 7
# MITOCHONDRIAL DYSFUNCTION-INDUCED FOOD-AVOIDANCE IN PRMT-1-NULL MUTANTS

## Purposes

Since PRMT-1 is the only type I PRMT in *C. elegans*, and the null mutant worm of *prmt-1* is available unlike it is in mouse or fruit fly, it seems that *C. elegans* is an ideal animal model to study the physiological functions of asymmetric arginine dimethylation. Previously, we reported that the transcriptional factor and orthologue of FOXO-1, DAF-16 is a substrate of PRMT-1 in *C. elegans*, and the asymmetric arginine dimethylation of DAF-16 acts as an anti-ageing switch which antagonizes the inhibitory effect of phosphorylation on DAF-16 by AKT-1 (9). In current study, we discovered that PRMT-1 contributes to almost all the asymmetric arginine dimethylation formation on mitochondrial proteins in *C. elegans*, and the loss of PRMT-1-mediated arginine methylation resulted in compromised mitochondrial function and increased mitochondrial ROS generation and stress responses in *C. elegans*. Next, we searched for any phenotypic changes of *prmt-1* mutant worms that may be related to the mitochondrial dysfunction to further elucidate the physiological roles of asymmetric arginine dimethylation.

## Results

It is known that *C. elegans* interprets compromised mitochondrial function as xenobiotic or pathogen attack, and thereby tend to avoid food intake even if the food does not contain pathogenic bacteria (7, 8). To examine the behavioral response to the mitochondrial dysfunction caused by loss of asymmetric arginine dimethylation, we performed food-avoidance experiments. As shown in Figure 6A, *prmt-1(ok2710)* mutants exhibited a dispersed feeding behavior in contrast to wild-type N2. It should be noted that this phenotype was similar to that caused by depletion of *isp-1* (Figure 6A), which encodes a component of the mitochondrial complex III in the electron transport chain and loss-of-function mutant of *isp-1* has been shown to increase ROS production and activate $UPR^{mt}$ (8, 29, 30). To determine whether the food-avoidance phenotype of *prmt-1(ok2710)* mutants indeed results from mitochondrial dysfunction, we performed epistasis analysis with RNAi against surveillance genes, *inx-17 or thoc-2*, that has been identified to be involved in food-avoidance downstream of mitochondrial dysfunction (8). As expected, silencing *inx-17* or *thoc-2* in *prmt-1(ok2710)* mutants completely suppressed the food-avoidance phenotype (Figure 6B). These findings suggest that food-avoidance behavior of *prmt-1*-null mutants is attributed to mitochondrial dysfunction due to loss of asymmetric arginine dimethylation in mitochondria.

## Discussion

Food-avoidance exhibited by *C. elegans* represents for an innate defensive behavior when they encounter the pathogenic foods. Like depletion of other key proteins in mitochondria, loss of PRMT-1 resulted in food-avoidance when fed on even non-pathogenic bacteria lawn, indicating that *C. elegans* interprets the disruption of core cellular functions such as mitochondrial metabolism as pathogen attracts. Indeed, the expression levels of stress response genes related to innate immunity elevated in *prmt-1* mutant worms.

Since food-avoidance can be observed not only when mitochondrial function is compromised, but also with defects in other core cellular functions, such as endoplasm reticulum, translation, or cytoplasmic protein folding. The results that silencing the mitochondria-specific surveillance genes in *prmt-1* mutant worm blocked the food-avoidance behavior confirmed that the phonotype is attributed to the mitochondrial dysfunction. Actually, these mitochondria-specific surveillance genes were identified as being able to block the $UPR^{mt}$, and our results further proved that $UPR^{mt}$ is the upstream molecular event of mitochondria-related food-avoidance.

However, the relation between elevated mitochondrial ROS and food-avoidance in *prmt-1* mutant worms remains to be investigated in the following study.

Figure 7-1

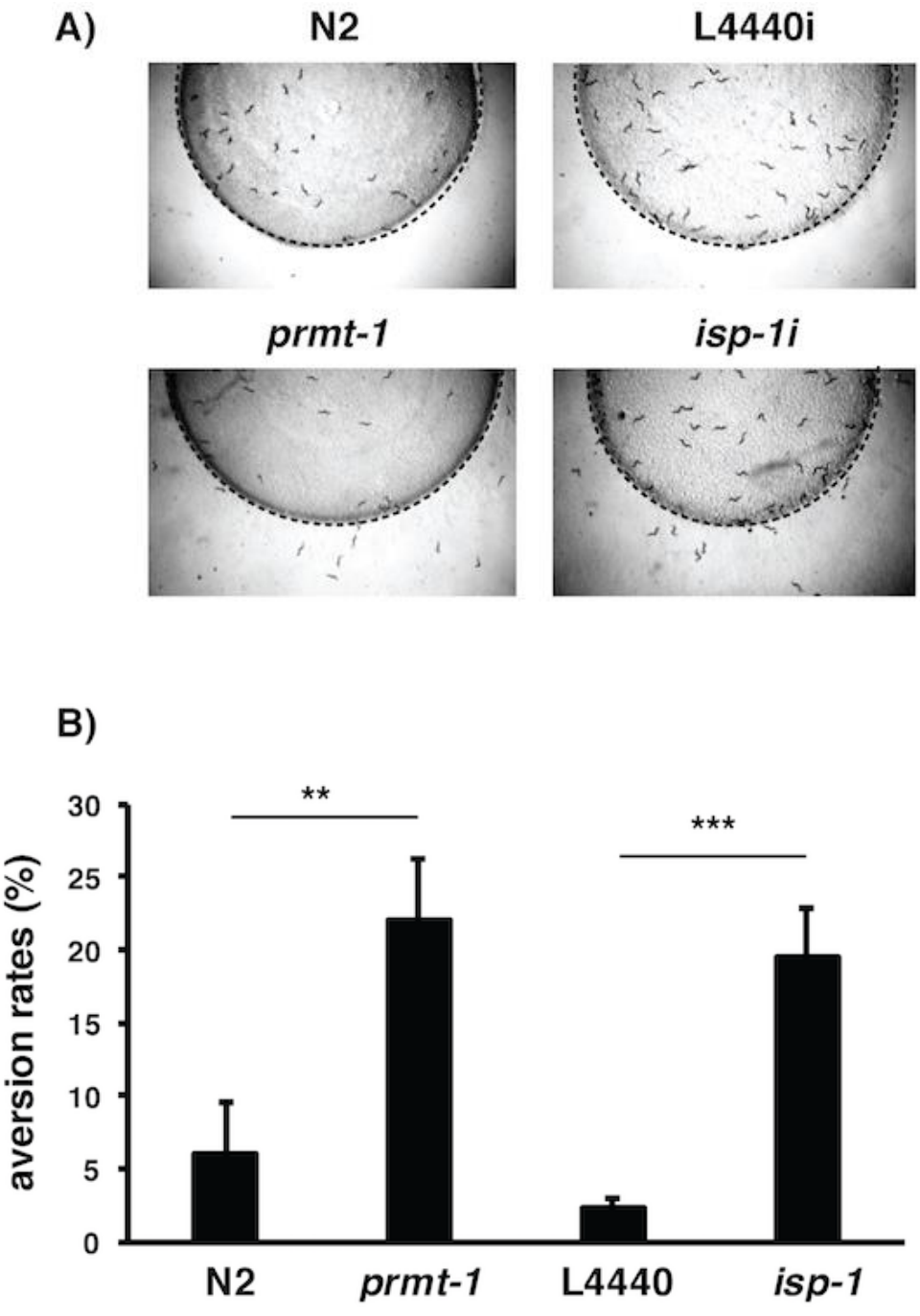


(legend on the next page)

Figure 7-1. Loss of enzymatic activity of *prmt-1* induces food avoidance behavior. (A) *prmt-1* mutant and *isp-1* knockdown worms exhibit food avoidance behavior in contrast to controls. Representative images of N2 or *prmt-1* mutants (left), and N2 fed on control L4440 or *isp-1* RNAi plates (right) are shown. (B) The quantified results of the food avoidance phenotype in (A) are shown. Error bars indicate ± SEM of three independent experiments. *n.s.* $p > 0.05$, *$p < 0.05$, **$p < 0.01$, ***$p < 0.001$.

Figure 7-2

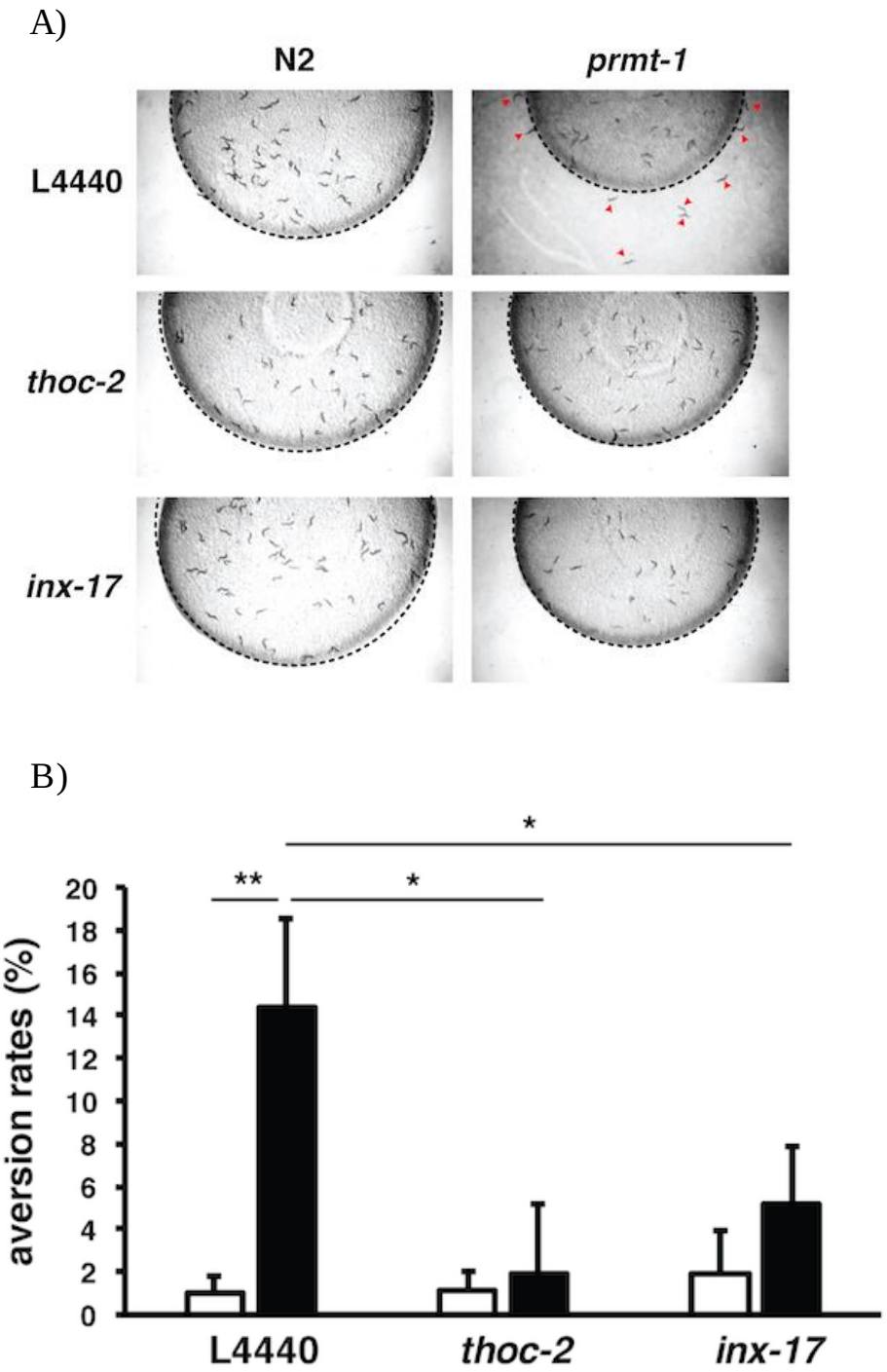


(legend on the next page)

Figure 7-2. Loss of prmt-1 induces food-avoidance mediated by mitochondrial stress. (A) The food avoidance phenotype exhibited in *prmt-1* mutants is suppressed by silencing of surveillance genes for mitochondrial stress. Representative images of N2 or *prmt-1* mutants fed on control L4440, *inx-17*, or *thoc-2* RNAi plates are shown. Arrowheads. (B) The quantified results of the food avoidance phenotype in (A) are shown. Error bars indicate ± SEM of three independent experiments. *n.s.* $p > 0.05$, *$p < 0.05$, **$p < 0.01$, ***$p < 0.001$.

# CHAPTER 8
## SUMMARY

In this study, we used *C. elegans* as a suitable multi-cellular model for screening *in vivo* substrates of PRMT-1 with the strategy of 2-D proteomic analysis based on Western blot against two distinct ADMA antibodies (Figure 3-1). We identified nine proteins modified by asymmetric arginine dimethylation *in vivo* (Figure 3-3 and Table 1). Of nine substrates, a nuclear receptor NHR-12 isoform c is the ortholog of mammalian HNF4γ that has been known to be regulated by PRMT1 in a methylation-dependent manner (33). Additionally, the identification of ribosomal RPL-4 and RPS-4 leads us to assume a similarity to recent findings that arginine methylation of mammalian RPS2 and RPS3 are involved in ribosomal assembly and biogenesis (34–36). Thus, our present results raise the possibility that asymmetric arginine dimethylation may play indispensable roles in transcriptional and translational regulation spanning a wide range of organisms.

An elusive issue should be addressed is where PRMT-1 binds to and methylates the three mitochondrial proteins (Figure 4-1 and 4-2) identified in the 2-D proteomic study (Figure 3-3 and Table 1). Furthermore, loss of PRMT-1 abolishes almost all the ADMA formation in mitochondria (Figure 4-4). Together, these results demonstrate that PRMT-1 is the responsible enzyme for asymmetric arginine dimethylation on mitochondrial proteins. Based on this

finding, *C. elegans* should be an ideal model for investigating whether the bulk asymmetric arginine dimethylation contributes to mitochondrial functions.

Intriguingly, as demonstrated by the subcellular fractionation (Figure 4-3), PRMT-1 is not localized in the mitochondria of *C. elegans* and we have also observed a similar result in human cells (data not shown). These results suggest that, unlike other posttranslational modifications such as phosphorylation and acetylation (11, 12), asymmetric arginine dimethylation of mitochondrial proteins doesn't occur within the mitochondria. Alternatively, given that over 99% of mitochondrial proteins are encoded by nuclear genome, they appear to be methylated simultaneously with translation in the cytoplasm before mitochondrial import. If so, it would add another layer of regulation to mitochondrial homeostasis potentially by modulating the transport of mitochondrial proteins in response to the intracellular environment.

Loss of asymmetric arginine dimehtylation in mitochondria results in decreased ATP synthesis activity (Figure 5-5). It is notable that ATP-2, a key component of ATP synthase, is identified as a substrate of PRMT-1 in current study. Remarkably, a global mass spectrometric analysis of *Trypanosoma brucei*, an early branching single-cell eukaryote, has reported that 54 and 13 mitochondrial proteins are asymmetrically and symmetrically dimethylated, respectively, and many of them are implicated in OXPHOS function (25). Considering these data together with our current findings, impairment in ATP synthesis of the *prmt*-1-null mitochondria may be attributed to loss-of

asymmetric arginine dimethylation on overall mitochondrial substrate proteins including ATP-2. In this meaning, our study for the first time bridged the asymmetric arginine dimethylation of mitochondrial proteins to fundamental mitochondrial function.

We provided evidence that enzymatic activity of PRMT-1 contributes to suppress mitochondrial ROS generation (Figure 6-1) probably by maintaining the OXPHOS function, while knockdown of PRMT-5, the major type II arginine methyltransferase in *C. elegans* (Kanou, *et al.* submitted), had no effect on that function (Figure 6-2). These results imply that symmetric arginine dimethylation at least by PRMT-5 is not necessary for normal OXPHOS function. However, instead of PRMT-5, non-canonical methyltransferase NDUFAF7 included in the matrix of mitochondria has been shown to methylate NDUFS2, a subunit of mitochondrial complex I, and thereby serve to assemble complex I (14), suggesting that, unlike asymmetric, symmetric arginine dimethylation on mitochondrial proteins are regulated by previously unidentified type II arginine methyltransferase(s) localized in mitochondria. Further investigations are needed to determine the functional difference between asymmetric and symmetric arginine dimethylation on mitochondrial proteins.

As a behavioral response to the mitochondrial dysfunction of *prmt-1*-null mutants, we observed food avoidance behavior (Figure 7-1) that is thought to be a defensive phenotype to protect core cellular functions including mitochondrial

respiration (7); because *C. elegans* living in microbe-rich environment is persistently attacked by pathogenic bacteria with their mitochondria easily targeted as valuable source of iron (37, 38). Meanwhile, despite that food does not contain pathogenic bacteria, mitochondrial dysfunction leads to food avoidance behavior, possibly by interpreting the mitochondrial defects as pathogen attack (8). In agreement with this idea, we found up-regulation of genes involved in xenobiotic-detoxification and natural immune response in *prmt-1*-null mutants (Figure 6-3). Furthermore, genetic analysis demonstrated that food-avoidance of *prmt-1*-null mutants can be blocked by silencing either *thoc-2* or *inx-17* (Figure 7-2), both of which have been recently identified as mitochondrial surveillance genes (8). THOC-2 has been shown to be an mRNA-binding protein facilitating nuclear export of mRNA and required for proper neuronal development (39), while the function of INX-17, which expresses abundantly in interneurons, is still unknown. Although the detailed mechanisms underlying food avoidance by mitochondrial dysfunction remain unclear, it is possible that loss of asymmetric arginine dimethylation induces this defensive behavior through the same pathway and neuronal circuits as that induced by inhibition of OXPHOS components (e.g. *isp-1*) because of the stress responses triggered by them are similar (28–30). Importantly, the depletion of *atp-2* or *hsp-60* in *C. elegans* induces $UPR^{mt}$ (18, 40) and food-avoidance behavior (7), strongly indicating that PRMT-1 serves as a positive regulator of mitochondrial function by methylating its substrates including ATP-2 and HSP-60.

In conclusion, we identified *in vivo* substrates of *C. elegans* PRMT-1 at the whole-body level. This is the first evidence that links asymmetric arginine dimethylation of mitochondrial proteins to ATP synthesis activity and mitochondrial homeostasis. Our study adds new evidence to the diverse regulations of mitochondrial proteins by post-translational modifications. It is speculated that arginine methylation, like phosphorylation or acetylation, may represent for a strategy employed by eukaryotic cells to regulate the mitochondria, originally engulfed as α-proteobacteria (2), to meet the cellular energy demands.

# REFERENCE

1. **Bedford MT**, **Richard S**. 2005. Arginine methylation an emerging regulator of protein function. Mol Cell **18**:263–72.

2. **Boisvert F-M**, **Chénard CA**, **Richard S**. 2005. Protein interfaces in signaling regulated by arginine methylation. Sci STKE **2005**:re2.

3. **Bedford MT**. 2007. Arginine methylation at a glance. J Cell Sci **120**:4243–4246.

4. **Nicholson TB**, **Chen T**, **Richard S**. 2009. The physiological and pathophysiological role of PRMT1-mediated protein arginine methylation. Pharmacol Res **60**:466–74.

5. **Bedford MT**, **Clarke SG**. 2009. Protein arginine methylation in mammals: who, what, and why. Mol Cell **33**:1–13.

6. **Tang J**, **Kao PN**, **Herschman HR**. 2000. Protein-arginine methyltransferase I, the predominant protein-arginine methyltransferase in cells, interacts with and is regulated by interleukin enhancer-binding factor 3. J Biol Chem **275**:19866–19876.

7. **Pawlak MR**, **Scherer CA**, **Chen J**, **Michael J**, **Ruley HE**. 2000. Arginine N -Methyltransferase 1 Is Required for Early Postimplantation Mouse Development , but Cells Deficient in the Enzyme Are Viable Arginine N -Methyltransferase 1 Is Required for Early Postimplantation Mouse Development , but Cells Deficient in the E. Mol Cell Biol **20**:4859–4869.

8. **Kimura S**, **Sawatsubashi S**, **Ito S**, **Kouzmenko A**, **Suzuki E**, **Zhao Y**, **Yamagata K**, **Tanabe M**, **Ueda T**, **Fujiyama S**, **Murata T**, **Matsukawa H**, **Takeyama K ichi**, **Yaegashi N**, **Kato S**. 2008. Drosophila arginine methyltransferase 1 (DART1) is an ecdysone receptor co-repressor. Biochem Biophys Res Commun **371**:889–893.

9. **Takahashi Y**, **Daitoku H**, **Hirota K**, **Tamiya H**, **Yokoyama A**, **Kako K**, **Nagashima Y**, **Nakamura A**, **Shimada T**, **Watanabe S**, **Yamagata K**, **Yasuda K**, **Ishii N**, **Fukamizu A**. 2011. Asymmetric arginine dimethylation determines life span in C. elegans by regulating forkhead transcription factor DAF-16. Cell Metab **13**:505–516.

10. **Quirós PM**, **Mottis A**, **Auwerx J**. 2016. Mitonuclear communication in homeostasis and stress. Nat Rev Mol Cell Biol **17**:213–226.

11. **Baker BM**, **Haynes CM**. 2011. Mitochondrial protein quality control during biogenesis and aging. Trends Biochem Sci **36**:254–261.

12. **Pellegrino MW**, **Nargund AM**, **Haynes CM**. 2013. Signaling the mitochondrial unfolded protein response. Biochim Biophys Acta **1833**:410–416.

13. **Haynes CM**, **Fiorese CJ**, **Lin YF**. 2013. Evaluating and responding to mitochondrial dysfunction: The mitochondrial unfolded-protein response and beyond. Trends Cell Biol **23**:311–318.

14. **Nargund AM**, **Pellegrino MW**, **Fiorese CJ**, **Baker BM**, **Haynes CM**. 2012. Mitochondrial Import Efficiency of ATFS-1 Regulates Mitochondrial UPR Activation. Science **337**:587–590.

15. **Melo JA**, **Ruvkun G**. 2012. Inactivation of conserved C. elegans genes engages pathogen- and xenobiotic-associated defenses. Cell **149**:452–466.

16. **Liu Y**, **Samuel BS**, **Breen PC**, **Ruvkun G**. 2014. Caenorhabditis elegans pathways that surveil and defend mitochondria. Nature **508**:406–410.

17. **Stensmyr MC**, **Dweck HKM**, **Farhan A**, **Ibba I**, **Strutz A**, **Mukunda L**, **Linz J**, **Grabe V**, **Steck K**, **Lavista-Llanos S**, **Wicher D**, **Sachse S**, **Knaden M**, **Becher PG**, **Seki Y**, **Hansson BS**. 2012. A conserved dedicated olfactory circuit for detecting harmful microbes in drosophila. Cell **151**:1345–1357.

18. **Rubio-Godoy M**, **Aunger R**, **Curtis V**. 2006. Serotonin - A link between disgust and immunity? Med Hypotheses **68**:61–66.

19. **Pagliarini DJ**, **Dixon JE**. 2006. Mitochondrial modulation: Reversible phosphorylation takes center stage? Trends Biochem Sci **31**:26–34.

20. **Baeza J**, **Smallegan MJ**, **Denu JM**. 2016. Mechanisms and Dynamics of Protein Acetylation in Mitochondria. Trends Biochem Sci **41**:231–244.

21. **Anderson K a**, **Hirschey MD**, **Matthew D**. 2012. Mitochondrial protein acetylation regulates metabolism. Essays Biochem **52**:23–35.

22. **Rhein VF**, **Carroll J**, **Ding S**, **Fearnley IM**, **Walker JE**. 2013. NDUFAF7 methylates arginine 85 in the NDUFS2 subunit of human complex i. J Biol Chem **288**:33016–33026.

23. **Zurita Rendon O**, **Silva Neiva L**, **Sasarman F**, **Shoubridge EA**. 2014. The arginine methyltransferase NDUFAF7 is essential for complex I assembly and early vertebrate embryogenesis. Hum Mol Genet **23**:5159–5170.

24. **Dhar S**, **Vemulapalli V**, **Patananan AN**, **Huang GL**, **Di Lorenzo A**, **Richard S**, **Comb MJ**, **Guo A**, **Clarke SG**, **Bedford MT**. 2013. Loss of the major Type I arginine methyltransferase PRMT1 causes substrate scavenging by other PRMTs. Sci Rep **3**:1311.

25. **Yoneda T**, **Benedetti C**, **Urano F**, **Clark SG**, **Harding HP**, **Ron D**. 2004. Compartment-specific perturbation of protein handling activates genes encoding mitochondrial chaperones. J Cell Sci **117**:4055–4066.

26. **Vigneswara V**, **Lowenson JD**, **Powell CD**, **Thakur M**, **Bailey K**, **Clarke S**, **Ray DE**, **Carter WG**. 2006. Proteomic identification of novel substrates of a protein isoaspartyl methyltransferase repair enzyme. J Biol Chem **281**:32619–29.

27. **Palikaras K**, **Lionaki E**, **Tavernarakis N**. 2015. Coordination of mitophagy and mitochondrial biogenesis during ageing in C. elegans. Nature **521**:525–528.

28. **Boisvert F-M**, **Côté J**, **Boulanger M-C**, **Richard S**. 2003. A proteomic analysis of arginine-methylated protein complexes. Mol Cell proteomics **2**:1319–30.

29. **Fisk JC**, **Li J**, **Wang H**, **Aletta JM**, **Qu J**, **Read LK**. 2013. Proteomic analysis reveals diverse classes of arginine methylproteins in mitochondria of trypanosomes. Mol Cell proteomics **12**:302–11.

30. **Hashimoto M**, **Murata K**, **Ishida J**, **Kanou A**, **Kasuya Y**, **Fukamizu A**. 2016. Severe Hypomyelination and Developmental Defects Are Caused in Mice

Lacking Protein Arginine Methyltransferase 1 (PRMT1) in the Central Nervous System. J Biol Chem **291**:2237–2245.

31. **Teyssier C**, **Ma H**, **Emter R**, **Kralli A**, **Stallcup MR**. 2005. Activation of nuclear receptor coactivator PGC-1alpha by arginine methylation. Genes Dev **19**:1466–1473.

32. **Yang W**, **Hekimi S**. 2010. A mitochondrial superoxide signal triggers increased longevity in caenorhabditis elegans. PLoS Biol **8**:e1000556.

33. **Yee C**, **Yang W**, **Hekimi S**. 2014. The intrinsic apoptosis pathway mediates the pro-longevity response to mitochondrial ROS in C elegans. Cell **157**:897–909.

34. **Xu S**, **Chisholm AD**. 2014. C.elegans epidermal wounding induces a mitochondrial ROS burst that promotes wound repair. Dev Cell **31**:48–60.

35. **Haynes CM**, **Petrova K**, **Benedetti C**, **Yang Y**, **Ron D**. 2007. ClpP Mediates Activation of a Mitochondrial Unfolded Protein Response in C. elegans. Dev Cell **13**:467–480.

36. **Berendzen KM**, **Durieux J**, **Shao L**, **Wolff S**, **Liu Y**, **Dillin A**. 2016. Neuroendocrine Coordination of Mitochondrial Stress Signaling and Proteostasis. Cell **166**:1553–1563.

37. **Barrero MJ**, **Malik S**. 2006. Two Functional Modes of a Nuclear Receptor-Recruited Arginine Methyltransferase in Transcriptional Activation. Mol Cell **24**:233–243.

38. **Swiercz R**, **Person MD**, **Bedford MT**. 2005. Ribosomal protein S2 is a substrate for mammalian PRMT3 (protein arginine methyltransferase 3). Biochem J **386**:85–91.

39. **Choi S**, **Jung CR**, **Kim JY**, **Im DS**. 2008. PRMT3 inhibits ubiquitination of ribosomal protein S2 and together forms an active enzyme complex. Biochim Biophys Acta - Gen Subj **1780**:1062–1069.

40. **Shin HS**, **Jang CY**, **Kim HD**, **Kim TS**, **Kim S**, **Kim J**. 2009. Arginine methylation of ribosomal protein S3 affects ribosome assembly. Biochem Biophys Res Commun **385**:273–278.

41. **Félix M-A**, **Duveau F**. 2012. Population dynamics and habitat sharing of natural populations of Caenorhabditis elegans and C. briggsae. BMC Biol **10**:59.

42. **Samuel BS**, **Rowedder H**, **Braendle C**, **Felix MA**, **Ruvkun G**. 2016. Caenorhabditis elegans responses to bacteria from its natural habitats. Proc Natl Acad Sci U S A **113**:E3941–E3949.

43. **Kumar R**, **Corbett MA**, **Van Bon BWM**, **Woenig JA**, **Weir L**, **Douglas E**, **Friend KL**, **Gardner A**, **Shaw M**, **Jolly LA**, **Tan C**, **Hunter MF**, **Hackett A**, **Field M**, **Palmer EE**, **Leffler M**, **Rogers C**, **Boyle J**, **Bienek M**, **Jensen C**, **Van Buggenhout G**, **Van Esch H**, **Hoffmann K**, **Raynaud M**, **Zhao H**, **Reed R**, **Hu H**, **Haas SA**, **Haan E**, **Kalscheuer VM**, **Gecz J**. 2015. THOC2 Mutations Implicate mRNA-Export Pathway in X-Linked Intellectual Disability. Am J Hum Genet **97**:302–310.

44. **Lin Y-F**, **Schulz AM**, **Pellegrino MW**, **Lu Y**, **Shaham S**, **Haynes CM**. 2016. Maintenance and propagation of a deleterious mitochondrial genome by the mitochondrial unfolded protein response. Nature **533**:416–419.

45. **Nunnari J, Suomalainen A.** 2012. Mitochondria: in sickness and in health. **Cell** 148: 1145-1159.

46. **Ventura N, Rea SL, Testi R.** 2006. **Exp. Gerontol.** 41: 974-991.